2010

Ozone-Based Decolorization of Food Colorants: Characterization and Application to Fruit Leather Recycling

Wenda Zhu
Iowa State University

Ozone-Based decolorization of food colorants: Characterization and application to fruit leather recycling

by

Wenda Zhu

A thesis submitted to the graduate faculty

in partial fulfillment of the requirements for the degree of

MASTER OF SCIENCE

Major: Toxicology

Program of Study Committee:

Jacek A. Koziel, Co-major Professor

J. (Hans) van Leeuwen, Co-major Professor

Byron F. Brehm-Stecher

Iowa State University

Ames, Iowa

2010

TABLE OF CONTENTS

Abstract

The commercial production of fruit leathers results in some material that is not to specification. Although this product remains edible and contains valuable ingredients such as fruit pulp, sugars and acidulates, it is not salable and its disposal is costly. Because these products are typically highly colored, recovery of fruit leather for recycling into the product requires colorant removal to avoid an unappetizing brownish color from the mixture of colorants. This research introduces a novel approach utilizing ozonation for color removal. The treatment was first applied to pure solutions of the commonly used food colorants 2-naphthalenesulfonic acid (Red 40), tartrazine (Yellow 5), and erioglaucine (Blue 1). Color removal was measured by UV/Vis spectrometer, and a Hunter colorimeter. Byproducts from ozone-based colorant decomposition were identified and quantified with SPME-GC-MS. Removal of Yellow 5, Red 40 and Blue 1 was about 65%, 80% and 90% complete, respectively, with 70 g ozone applied to 1 kg aqueous fruit leather suspension solution. Given the known structures of these dyes, a concern with this approach is the potential formation of toxic ozonolysis byproducts. In initial work, carbonyl compounds were identified as major byproducts. Among these, benzaldehyde, 2-furfural, ethanal and hexanal were identified as byproducts of known toxicity at levels sufficient for concern. A head-space solid-phase microextraction (HS-SPME) method with on-fiber derivatization using o-(2,3,4,5,6-pentafluorobenzyl)hydroxylamine hydrochloride (PFBHA) was optimized for detection and quantification of carbonyl compounds in ozonated fruit leather suspensions. Ethanal, hexanal, furfural and benzaldehyde were quantified with the newly developed method, and detection limits were in the range of 0.016 – 0.030 µg/L. For furfural, the ozonolysis byproduct noted in the literature as having the highest median lethal dose value, the maximum amount generated

was determined to be under the detection limit, 0.016 μg/L of 100% fruit leather solution/suspension, while hexanal was the most abundantly generated, at 80.0 ± 22.0 mg/L. A conservative risk assessment based on published toxicity information for the main ozonolysis products generated in this study suggests the acceptability of ozone-based decolorization in fruit leather recycling. A preliminary cost estimate suggests a potential $0.25 million annual profit on recycling a 1,000 tons of waste fruit leathers per year.

Chapter 1. Introduction

Fruit leathers are a popular snack food containing fruit pulp, sugars and food-grade colorants and are produced at rates of tons per hour in the US. As with any food, the commercial production of fruit leathers results in some material that is not to specification. Disposal of this material is costly, as it remains edible and contains valuable ingredients such as fruit pulp, sugars and acidulates. Recovery of out of specification fruit leather for product rework (recycling) requires colorant removal to avoid an unappetizing brownish color resulting from compositing leathers of different colors. The food colorants studied here were Red 40, an acidic and azoic synthetic colorant; Yellow 5, an azoic synthetic colorant; and Blue 1, a synthetic colorant. Colorant removal is often achieved by oxidation processes (Forgacs et al., 2004). These could include ozonation, or Advanced Oxidation Processes (AOPs) for decolorization, including photocatalytic oxidation, electrochemical treatment, or ozonation combined with ultraviolet (UV) radiation or ultrasonication. Non-oxidative decolorization methods can be adsorption, biodegradation, coagulation and ultrasonic irradiation (Aksu et al., 2008; Fu et al., 2001; Forgacs et al., 2004).

For food-based applications, it is ideal that the implemented decolorization process is free of additive residue from decolorization reagents. In the processes of adsorption, electrochemical oxidation, biodegradation and coagulation, addition of solid reagents is necessary. Activated carbon (charcoal) is the most widely used adsorbent, with high adsorption capacity (Richardson et al., 2008), while fly ash, waste red mud, biomass, and clay minerals are substituted as less expensive adsorbents (Hamdaoui et al., 2006; Ozsoy et al., 2008a; Vimonses et al., 2009). Non-viable plant or microbial cells are additional choices as sorbent, which interact with the impurity

through adsorption, deposition, and ion-exchange (Ozsoy et al., 2010a; Aksu et al., 2008). Electrochemical oxidation uses electrolytes such as sodium chloride (Maljaei et al., 2009) or ferrous sulfate (Villanueva-Rodríguez et al., 2009) to enhance conductivity, while a low voltage direct current is applied to oxidize colorants. Unsatisfactory decolorizing efficiency has been reported for azoic and acid colorants using biodegradation and coagulation processes (Richardson et al., 2008), and Yellow 5 and Red 40 are such colorants. Photocatalytic oxidation processes produce oxidative radicals, requiring a catalyst such as TiO_2 as an additional semiconductor phase (Tang et al., 1995a and b; Ao et al., 2007). Oxidative radicals can also be generated from ultrasonic irradiation of oxygen and water (Ghodbane et al., 2009), and this technique can be applied together with ozonation (Zhang et al., 2006). However, a main drawback of the techniques listed above is that they involve addition to the food of reagents or additives that subsequently must be removed or recovered, which involves additional processing. In contrast, ozone-based decolorization has many potential advantages as a means for processing of industrial food materials, as it is highly effective, does not generate solid wastes and is residue-free (Ozsoy et al., 2008b; Wu et al., 2008). Additionally, selective ozonation of specific compounds is possible, even in the presence of other organic substances (van Leeuwen et al., 2009a and b).

Ozone-based decolorization has been studied combined with other techniques such as ultrasonic irradiation (Zhang et al., 2006), UV catalysis (Hsing et al., 2007), or membrane filtration (Wu et al., 1998). The use of ozone-based oxidative treatment started from early 1900s, and has been widely utilized in the food industry (Guzel-Seydim et al., 2004). Ozone-based oxidation has previously been shown to be selective and effective enough for colorant

degradation (Wu et al., 2008 and Ozsoy et al., 2008b). Combination of ozonation with other AOP techniques is expected to result in a higher oxidative potential (Glaze et al., 1982; Koyuncu et al., 1996 and Hsing et al., 2007) and lower selectivity in complex systems (Koyuncu et al., 1996). Ozone is commonly used in wastewater (van Leeuwen et al., 2003a) and water treatment (van Leeuwen et al., 2003b). Considering the equipment costs for the scale needed in this study, along with treatment effectiveness and process selectivity, ozonation treatment alone was expected to serve as an attractive solution for color removal in this study. However, a major concern in this study was the generation of unwanted byproducts from ozonolytic degradation of the food colorants used here. Common structural elements of colorants such as Yellow 5, Red 40 and Blue 1 include azo bonds and benzene rings. Different breakdown mechanisms of these groups have been observed in different decolorization processes, with the azo bonds being most subject to cleavage (table 1.2). The ring structures can be left intact, opened or mineralized during decolorization. Some colorants were found to degrade in the natural environment without cleavage of their benzene rings (Colombini et al., 2007; Grosjean et al., 1992; Huang et al., 2009; Gosseti et al., 2004, 2005 and 2008). Other dyes, such as morin, a textile dye with a flavone backbone, have been shown to break down at ambient oxygen levels, with a reaction catalyzed by visible light (Colombini et al., 2007). Grosjean et al. (1992) reported the fading of some organic artists' colorants by atmospheric nitric acid and breakdown of curcumin by ambient ozone. The photodegradation of food colorants in beverages has also been reported, notably, Blue 1 (Gosseti et al., 2007), azo dye Sunset Yellow FCF (Gosseti et al., 2005 and 2008) and Chromotrope FB-E122 (Gosseti et al., 2008). Decolorization of Blue 1 without opening of the benzene ring was found to be possible using potassium persulfate (Gosseti et al., 2004), and

selective enzymatic cleavage of the azo bond of Methyl Orange was observed in decolorization treatments using the bacterium *Kocuria rosea* (Gosetti et al., 2004). Ring-opening degradations were observed with Advanced Oxidation Processes (AOPs), such as UV/TiO_2 oxidation of anthraquinone dye Acid Blue 40 (Tang et al., 1995), Co^{2+}/ peroxymonosulfate oxidation of the azo dye Reactive Black B (Huang et al., 2009) and electrochemical oxidation of the azo dye C.I. Reactive Yellow 3 (Maljaei et al., 2009). Although the azo dye Acid Orange could not be effectively degraded using UV/TiO_2 treatment, an ozone dose of 50.7 mg/L·h^{-1} was found to completely mineralize this dye to nitrate and gaseous nitrogen compounds (Hsing et al., 2007). Mineralization of Acid Orange 6 was also possible using a Co^{2+}/peroxymonosulfate decolorization system (Chen et al., 2007). Processes capable of mineralization are of special interest, as they are expected to generate byproducts having the lowest toxicities. For example, some of the degradation products reported for mineralization of dyes are small molecules that do not contain benzene rings, or that have a lower degree of unsaturation, another parameter associated with lower toxicity. Previous studies have reported mineralization of colorants using ozone-based oxidation (Hsing et al., 2007), indicating the promise of this approach for decolorization of food dyes with minimal generation of unwanted byproducts.

Table 1.1. Dye decolorization processes reported in the literature.

Technique	**Colorant**	**Reagent**	**Reference**
Adsorption	Methylene Blue	Activated carbon	Karaca et al., 2008
	Blue 1, Red 40 and Yellow 5	Activated carbon	Ozsoy et al., 2010b
	Methylene Blue	Cedar sawdust and crushed brick	Hamdaoui et al., 2006
Biosorption	Gryfalan Black RL metal-complex dye	*Rhizopus arrhizus* and *Aspergillus niger*	Aksu et al., 2008
	Cu^{2+} ions	Dried *R. microsporus*	Ozsoy et al., 2008a
	Methylene Blue Orange II	Bacterial biomass	Van Leeuwen et al. 2009 a & b
Biodegradation	Methyl Orange	*Kocuria rosea*	Hamdaoui et al., 2006
Electrochemical oxidation	Reactive Yellow 3	Graphite and NaCl	Maljaei et al., 2009
	Acid Yellow 36	Boron-doped diamond and ferrous sulfate	Villanueva-Rodríguez et al., 2009

Table 1.1. continued.

Photocatalytic	Direct Blue 87, Reactive Red 120, Basic Yellow 15, Acid Blue 40 and Direct Blue 160	UV/TiO_2	Tang et al., 1995a
	Acid Blue 80	$UV\text{-}Vis/TiO_2$	Ao et al., 2007
	Acid Blue 40	UV/TiO_2	Tang et al., 1995b
Ultrasonic	Acid Blue 25	Carbon tetrachloride	Ghodbane et al., 2009
Ozonation	C.I. Reactive Blue 15	Ozone	Wu et al., 2008
	Blue 1, Red 40 and Yellow 5	Ozone (compared with adsorption and coagulation)	Ozsoy et al., 2008b
	Blue 1, Red 40 and Yellow 5	Ozone	This study

Table 1.2. Colorant degradation products reported from various decolorization processes.

Colorant	**Reagent**	**Degradation**	**Reference**
Morin	Ambient oxygen, light	Ring intact	Colombini et al., 2007
Alizarin, Alizarin crimson, Pararosaniline base, Basic fuchsin, Acridone, Quinacridone Red, Indigo, Thioindigo violet, Curcumin	Ambient nitric acid	Ring intact	Grosjean et al., 1992
Curcumin	Ambient ozone	Ring intact	Grosjean et al., 1998
Blue 1	Light	Ring intact	Gosseti et al., 2007
Sunset Yellow FCF	Light	Ring intact	Gosseti et al., 2005 and 2008
Chromotrope FB-E122	Light	Ring intact	Gosseti et al., 2008
Blue 1	Potassium persulfate	Ring intact	Gosseti et al., 2004
Methyl Orange	*Kocuria rosea*	Ring intact	Parshetti et al., 2010

Table 1.2. continued.

Acid Blue 40	UV/TiO_2	Ring opened	Tang et al., 1995
Reactive Black B	Co^{2+}/peroxymonosulfate	Ring opened	Huang et al., 2009
C.I. Reactive Yellow 3	Electrochemical oxidation	Ring opened	Maljaei et al., 2009
Acid Orange 6	Ozone	Mineralization	Hsing et al., 2007
Acid Orange 6	Co^{2+}/peroxymonosulfate	Mineralization	Chen et al., 2007
Blue 1, Red 40 and Yellow 5	Ozone	Mineralization	This study

In the present study, carbonyl compounds were identified as major byproducts from ozone-based decolorization during fruit leather recycling. Among the detected carbonyl compounds, ethanal (acetaldehyde), 2-furfural and benzaldehyde are of concern according to published toxicity data, while hexanal, a compound used in foods as a flavorant (used at 0.005 – 4 ppm to impart a fruit flavor), was found at a high level following ozonation, along with ethanal, which also has food uses as a flavor adjuvant. In other ozonolysis applications such as treatment of paper pulp and water, carbonyl compounds have also been found as major byproducts (Le Lacheur et al., 1993). Carbonyl compounds are common in the environment, and may be generated via various processes, including oxidative disinfection of drinking water (Bao et al.,

1998), incomplete combustion of fossil fuels, the burning of wood (Beránek et al., 2008) and ambient photochemical processes (Satsumabayashi et al., 1995). As with many compounds found in the environment, toxicity can arise during metabolism. Inside the human body, carbonyl groups can either be oxidized to a carboxyl group or reduced to a hydroxyl group, with oxidation being both dominant and irreversible (Sladek et al., 1989). Another metabolic pathway involves interaction between the carbonyl group and thiol or amine groups, which can lead to covalent crosslinking between DNA and proteins (DNA-protein, protein-protein, DNA-DNA) (Chaw et al., 1980; Feldman et al., 1978; Ma et al., 1988). These reactions may ultimately result in mutation and tumor formation, as studies on laboratory animals have shown (Cancho et al., 2001).

Carbonyl compounds are also reactive outside of the body, and must be derivatized for sampling (Le Lacheur et al., 1993). For example, Ortiz et al. used an annular denuder coated with o-(2,3,4,5,6-pentafluorobenzyl)hydroxylamine hydrochloride (PFBHA) for collection of biofunctional carbonyl compounds from ambient air (Ortiz et al., 2006). The captured aldehydes were then extracted using acetonitrile/CH_2Cl_2 for instrumental analysis. Solid phase extraction has also been coupled with PFBHA derivatization for the extraction of carbonyls from wine (Culleré et al. 2004). In a study on carbonyls from engine exhaust, 2,4-dinitrophenyl-hydrazine (DNPH) was used as the derivatization reagent coated onto silica gel cartridges (Pang et al., 2008).

A drawback of the methods described above is that they require laborious pre-analytical sample preparation. In contrast, solid phase microextraction (SPME) is a technique developed in recent years that integrates both sampling and sample preparation steps (Pawliszyn et al., 1997).

The technique has been successively applied for analysis of carbonyls in combination with PFBHA derivatization (Bao et al., 1998; Deng et al., 2004; Koziel et al., 2001). In the present study, SPME was found to be both sensitive and selective, in addition to being less labor intensive. In our ozonation process, ozone was generated at a constant known rate, with ozonation time being the only independent variable. Different ozonation times were expected to influence the generation of byproducts. We used SPME-GC-MS both with and without derivatization for the study of byproducts from the ozonolytic breakdown of food colorants.

Overall, we sought to test decolorization efficiency with UV/Vis spectrometer and Hunter colorimeter, to semi-quantitatively analyze non-carbonyls with non-derivatization SPME, to develop an on-fiber derivatization SPME method for the carbonyls with highest concern (ethanal, hexanal, 2-furfural and benzaldehyde), to use SPME methods to acquire byproduct generation profiles as a function of different ozonation times, and to use these time-product profiles to identify an effective decolorization regime resulting in minimal generation of undesirable byproducts.

Chapter 2. Experimental

2.1. Ozone treatment system

The ozonation system was set up according to figure 2.1.1 and 2.1.2. The 99.999% purity air in the air cylinder was the oxygen supplier for the TOG C2B corona discharge ozone generator (Triogen, Craigton, Glasgow, UK). Air was introduced into the ozone generator at a constant flow rate. The flow rate was measured by a GFC 37 mass flow controller (Aalborg, Orangeburg, New York, USA). Ozone was generated from air cylinder-delivered oxygen via corona discharge. A capillary grade hydrocarbon and moisture trap (Restek, Bellefonte, PA, USA) was connected to the air cylinder to reduce nitric acid formation from the corona discharge during ozone production. Under a constant airflow rate, the dosage of ozone generated is a direct function of time. Specific ozone doses were reached by controlling the ozonation time. Although parameters such as temperature and pH value in the system are known to influence the mass transfer of ozone and subsequent decolorization efficiency (Wu et al., 2001), costs associated with adjustment of these parameters in the real industrial process are another concern. Simple mass transfer enhancement may be achieved through the generation of microbubbles (Chu et al., 2007). In the present study, ozone was introduced to the bottom of a reactor vessel containing 200 mL of sample suspension (Figures 2.1.1 and 2.1.2). Ozone microbubbles were generated using a sintered glass sparger, while pH and temperature were not adjusted.

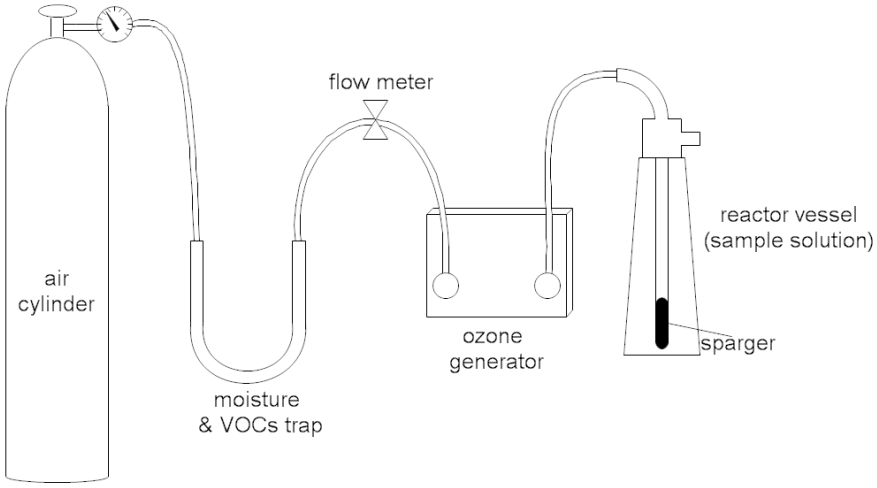

Figure 2.1.1. Schematic of the ozonation system used in this study

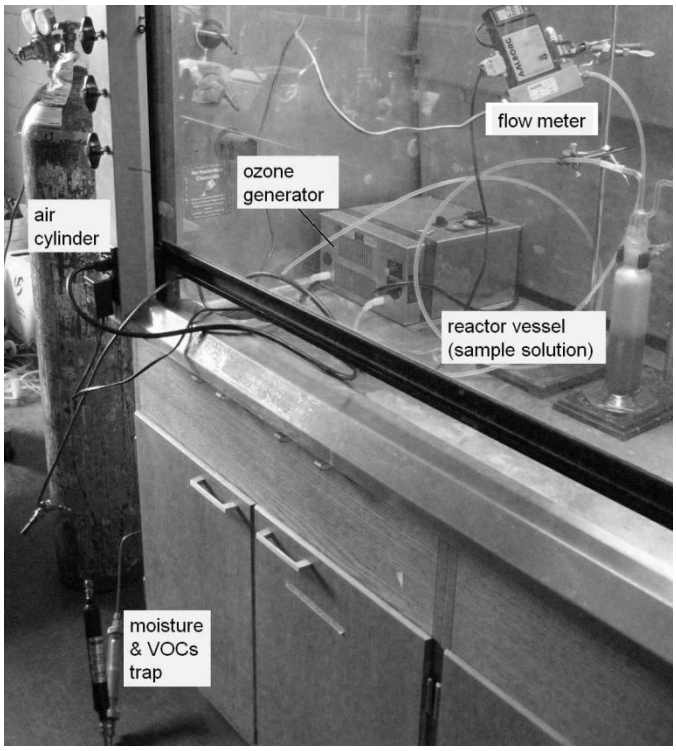

Figure 2.1.2. Photo of the ozonation system used in this study

2.2. Quantification of ozone dosage

Ozone dosage was calculated using a chemical titration method. A constant ozone dose was supplied by the corona discharge ozone generator, which used compressed air as the oxygen supply. Ozone/air gas was introduced at a constant flow rate through a glass tube from top to the bottom with a sintered glass sparger, and passed through 200 mL 2% potassium iodide solution in a vessel. After ozonation, dye solution was transferred to a 500 mL conical beaker, and 10 mL 2 M sulfuric acid solution was added and mixed into the solution (adapted from Clesceri et al., *Standard methods for the examination of water and wastewater*, 1998). This solution was left at room temperature in dark for 3 hours to release iodine from iodate as byproduct. The solution was then titrated with 0.05 M sodium thiosulfate. As yellow color almost disappeared, 2 mL 1% starch indicator was added, turning the solution blue. This titration process was repeated until the blue color was no longer formed.

In the ozone capturing process, iodate was generated from ozonation of iodine:

Iodide oxidation reaction

$$4 \cdot O_3 + 10 \cdot I^- \rightarrow H_2O_2 + 5 \cdot I_2 + 4 \cdot H_2O + 3 \cdot O_2$$

Side reactions

$$3 \cdot O_3 + I^- \rightarrow 3 \cdot O_2 + IO_3^-$$

$$5 \cdot O_3 + I_2 + H_2O \rightarrow 5 \cdot O_2 + 2 \cdot IO_3^- + 2 \cdot H^+$$

To reduce all iodate to ozone to iodine for titration, sulfuric acid was added to the ozonated KI solution:

Iodine release reaction

$$IO_3^- + 5\cdot I^- + 6\cdot H^+ \rightarrow 3\cdot I_2 + 3\cdot H_2O$$

After 3 hours of reaction in dark, iodate from iodide ozonation side reaction was found to be reduced thoroughly. A deeper orange color was observed after dropwise addition of sulfuric acid and storage.Ozone dose was calculated according to the summarized reactions as follows:

Total reaction

$$O_3 + 2\cdot I^- + H_2O \rightarrow I_2 + O_2 + 2\cdot OH^-$$

$$I_2 + 2\cdot S_2O_3^{2-} \rightarrow 2\cdot I^- + S_4O_6^{2-}$$

The calculation of ozone dose was as following:

$D_{ozone} = A \times N \times 24/T$

Where:

D_{ozone} = ozone dose, mg/min;

A = the amount of $Na_2S_2O_3$, mL;

N = the normality of $Na_2S_2O_3$, mol/L;

T = ozonation time, min;

24 = ozone molecular mass (48) divided by the ratio of $Na_2S_2O_3$ to ozone as reactants, $g\cdot mol^{-1}$.

2.3. Objective measurement of color removal

Objective color measurement was carried out with a SpectraMax Plus 384 UV/Vis spectrometer (Molecular Devices, Sunnyvale, CA, USA) and Hunter colorimeter (HunterLab, Reston, Virginia, USA). The UV/Vis spectrometer measures absorbance of light in a sample at a specified wavelength. Content of a colorant in solution can be determined by measuring its absorbance at its maximum absorbance wavelength, which is characteristic of each dye. The spectrometer was calibrated using distilled water as a blank prior to taking measurements. Aqueous solutions of indvidual colorants were transferred to individual cuvettes for measurement. For spectrophotometric measurements of fruit leather solution/suspension, the sample was centrifuged and filtered with a 2 μm filter paper (Whatman, Maidstone, Kent, UK) to remove colloidal particles before being transferred to a cuvette. Absorbance of each sample at its maximum absorbability wavelength was recorded as A_{max}.

The Hunter colorimeter was used to measure the color fruit leather solution/suspension without cleaning the sample. The color is expressed in the Hunter *L*,*a*,*b* Color Space, where *L* is on the lightness axis, 0 is black and 100 is white; *a* is on the red-green axis, positive is red and negative is green; *b* is on the blue-yellow axis, positive is yellow and negative is blue (Chutintrasri et al., 2007). The instrument was firstly calibrated with black and white reference tiles (L = 91.8; a = -0.8; b = 0.1). A plastic sample dish was filled to the top with sample solution/suspension so that an identical depth was achieved for each measurement. The dish was covered with a plastic dish cover and the measurement made. The three-color coordinates were recorded and total color difference, ΔE, was calculated based on the equation:

$$\Delta E = [\{L_0 - L)^2 + (a_0 - a)^2 + (b_0 - b)^2]^{1/2}$$

where L_0, a_0 and b_0 represent the readings from untreated fruit leather solution/suspension, and L, a and b represent those from sample treated with specific ozone dose.

2.4. Screening and identification of ozonolysis byproducts

Identification of byproducts was performed by a GC-MS analysis following direct immersion (DI) SPME with a 50/30 μm DVB/CAR/PDMS fiber, and on-fiber derivatization SPME with a 65 μm PDMS/DVB fiber. All SPME fibers and holders were purchased from Supelco (Bellefonte, PA, USA). The GC-MS system was Agilent 6890N GC system coupled with Agilent 5975C VL MSD. Colorant aqueous solution was used as the model system for identification of byproducts from colorant decomposition. The DI-SPME was performed by immersing a 50/30 μm DVB/CAR/PDMS fiber into a 30 mL treated/untreated colorant solution in a 40 mL vial for 30 min at room temperature with 800 rpm stirring. The fruit leather solution/suspension samples were also analyzed by headspace (HS)-SPME, and the trend of aliphatic acid content against ozone dose was monitored. A 50/30 μm DVB/CAR/PDMS fiber was exposed to the headspace of 10 mL sample in a 40 mL vial for 60 min at room temperature, with 800 rpm stirring. Sample extracted by the 50/30 μm DVB/CAR/PDMS fiber was analyzed by a 60 m polar BP-21 column in GC-MS. Injector was at 250 °C. The oven temperature started from 40 °C initially, holding 5 min and then raise to 220 °C at 4.5 °C/min, followed by a 5 min hold. Helium was used as the carrier gas at a flow rate of 1.7 mL/min. The mass-to-charge ratio (m/z) range was set

between 29 and 280. Spectra were collected at 6 scans/s and electron multiplier voltage was set to 1500 V. The screening and identification results were the basis to select target compounds.

2.5. Quantitative analysis of carbonyls present in pure dye or ozonated fruit leather solution/suspension

2.5.1. Response Factor Calculation

The evaluation of extraction efficiency requires transferring the response of each chemical in the GC-MS system to its mass extracted by on-fiber derivatization in SPME. Dividing the peak area count of a carbonyl at known amount by its mass gives the response factor of the specific chemical.

Response factor = peak area count of oxime (isomers)/*mass* (ng) of injected derivatized carbonyl

To obtain carbonyl derivatives for response factor calculation, a specific amount of carbonyl compound was spiked to PFBHA methanol solution for reaction. The molar concentration of PFBHA solution was 10 times higher than that of the carbonyl compound to ensure a quantitative reaction, and the reaction was carried out in the dark at room temperature for at least 2 h (Bao et al., 1998). After derivatization, the solution was quantitatively introduced into the GC-MS system by direct injection. The response factor of each carbonyl compound was obtained from dividing the peak area count of the derivative by the injection mass of the chemical.

2.5.2. PFBHA Doping of SPME Fiber

In application with SPME, DNPH and hydroxymethyl piperidine (HMP) were found to generate a number of byproduct peaks, while PFBHA was found to be the ideal derivatization reagent for SPME analysis (Martos et al., 1998). For direct derivatization, at least 30 min of derivatization reaction is required in a diluted system (Bao et al., 1998; Beránek et al. 2008; Saison et al., 2009). In the present study, an on-fiber derivatization method was used (Beránek et al., 2008; Deng et al., 2004; Koziel et al., 2001). In this process, the derivatization reagent is first doped onto the SPME fiber, and then the fiber coated with PFBHA is exposed to the headspace of the sample solution to react with carbonyl compounds. A 65 μm PDMS/DVB (poly-dimethylsiloxane/divinylbenzene) fiber was selected because it was found to retain a large amount of PFBHA after exposing to the ambient air (Martos et al., 1998). During both the doping and derivatization procedures, a 1 cm Teflon-coated stir bar was placed in the sample stirring at 800 rpm, and the vial was placed in a water bath set to a specific temperature (40, 60 or 80 ˚C, depending on the experiment). For PFBHA doping, a PDMS/DVB fiber was exposed to the headspace of 1 mL PFBHA aqueous solution for 15 min. Immediately after doping with PFBHA, the SPME fiber was introduced into the headspace of a sample solution, because immersing a PFBHA coated PDMS/DVB fiber into the sample solution was found to dissolve the PFBHA coating (Beránek et al., 2008). Headspace extraction was performed for a specific time. The doping procedure and on-fiber derivatization were both performed in the same thermal water bath at the same temperature.

Different PFBHA dopant solution concentrations, on-fiber derivatization times and sampling temperatures were tested. Derivatization efficiencies were evaluated according to the GC-MS response of carbonyl derivatives to determine the optimum SPME conditions.

2.5.3. GC-MS Condition for Carbonyl Analysis

Following on-fiber derivatization, the SPME fiber was introduced to the injection port of the GC instrument for thermal desorption. An Agilent 6890N GC system was equipped with Agilent 5975C VL MSD. Samples were analyzed in a 60 m × 0.32 mm × 0.25 μm SGE BP-21 column. The GC injection port temperature was 250 ˚C. The oven temperature was raised from 120 ˚C to 180 ˚C at a 4.5 ˚C/min ramp, and then ramped to 220 ˚C at 15 ˚C/min, holding for 3 min. Helium was the carrier gas, and the flow rate was 1.7 mL/min. The scanning range of the MS detector was m/z = 33 to 352. Temperatures of the MS source and MS quadrupole were 230 ˚C and 150 ˚C respectively. A selective ion monitoring (SIM) mode (table 2.5.1) was run simultaneously in total scanning mode for quantification.

Table 2.5.1. Selected scanning ions in the SIM

Carbonyl (-PFBHA Derivative)	**Significant Ions**	**Carbonyl (-PFBHA Derivative)**	**Significant Ions**
Ethanal	181 **209** 239	Octanal	181 **239** 323
Propanal	181 195 **223** 236	Acetone	181 223 **253**
Butanal	181 **239** 267	2-Heptanone	181 **253**
Pentanal	181 **239** 281	2-Furfural	181 248 **291**
Hexanal	114 181 **239** 295	Benzaldehyde	181 271 **301**

Note: Quantification ions are in bold.

2.5.4. Validation of the Method

Calibration curves of ethanal, hexanal, 2-furfural, and benzaldehyde were generated, and the gradient concentrations were in the range of 2 – 50 ng/mL, 20 – 8000 ng/mL, 0.04 – 0.8 ng/L, and 0.1 – 1.5 ng/mL respectively, corresponding to the chemical contents in the real sample. For limit of detection (LOD), and limit of quantification (LOQ) determinations, 0.1 µg/L spiked aqueous solutions were analyzed in 7 replicates. According to the US EPA, LOD = standard deviation of replicate analyses × Student's t-value for the 99% confidence level with n-1 degree of freedom, and LOQ = standard deviation of replicate analyses × 10 (US EPA, 1998).

Chapter 3. Results and Discussion

3.1. Ozone Generator Calibration

A considerable enhancement of linearity and precision of the iodometric titration for ozone quantification was observed with a 3 h iodine release procedure (table 3.1.1). The 3-h iodine release procedure was included in the following ozone quantification procedures. With a 500 mL/min air supply, knob setting at 1 (the lowest corona discharge frequency) was found to provide the required ozone generation level. The knob was set at 1 in the following measurement and treatment procedures. Ozone generator calibration curves were generated with air supply at 500 mL/min, and 800 mL/min (table 3.1.1).

Table 3.1.1. Optimization of iodometric titration for ozone quantification

Air Supply	**Calibration**	**Release Iodine**	**R^2**	**RSD (%)**		
(mL/min)	**Curve**	**for 3 h**		**Average**	**Intra-day**	**Inter-day**
500	$D_{ozone} = 3.898 \cdot T$	No	0.490	7.88	12.8 (n=4)	N/A
500	$D_{ozone} = 4.522 \cdot T$	Yes	0.988	2.94	4.74 (n=6)	4.50 (n=9)
800	$D_{ozone} = 6.644 \cdot T$	Yes	0.999	0.37	0.52 (n=3)	N/A

Note: The calibration curves were all forced to the intercept = 0. The knob setting was 1. In the equation, D_{ozone} is in mg/L of air flow, and T is in min. N/A: the value was not calculated.

3.2. Color Removal Efficiency

3.2.1. Colorant Solution as Model Sample

Working with pure aqueous solutions of each dye, decolorization curves were obtained by plotting $\log_A$ against the delivered ozone dosage. A pseudo first order colorant decomposition reaction was observed for each colorant (figure 3.2.2), which agrees with results from previous studies on ozone-based decolorization (Wu et al., 2001 and 2008). Among the three colorants studied, Blue 1 was found the most rapidly decomposed, followed by Red 40, then Yellow 5.

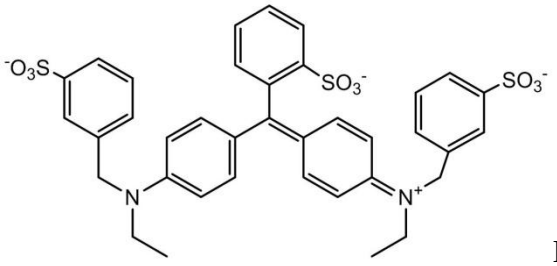

Blue 1

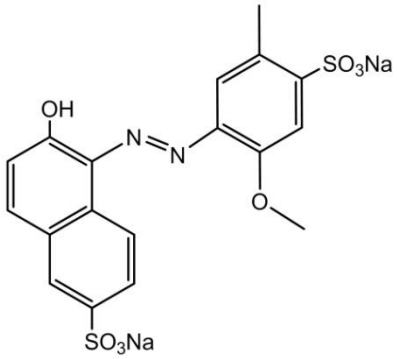

Yellow 5

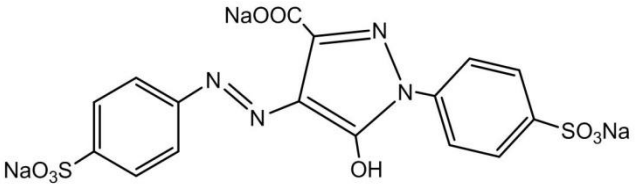

Red 40

Figure 3.2.1. Chemical structures of the food colorants (structures were drawn with ChemDraw).

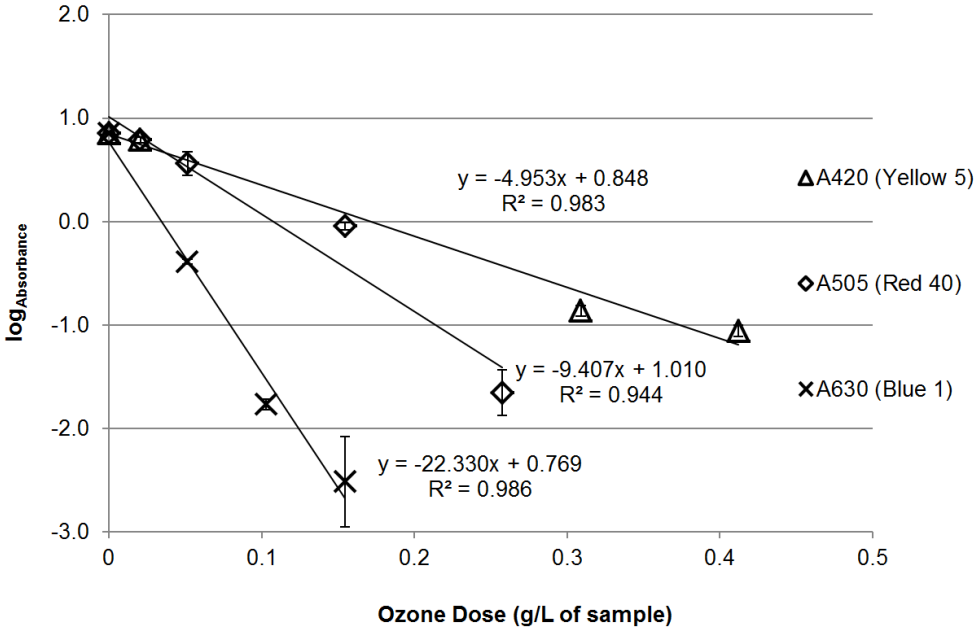

Figure 3.2.2. Color removal efficiency for different colorants. Each 200 mL aqueous solution of individual colorant was treated with 11.3 mg/L·min^{-1} of ozone.

3.2.2. Waste Fruit Leather Solution/Suspension

Increasing ozone doses, led to increased color removal. A pseudo-first order colorant degradation reaction was also observed in ozone treatment of the mixed colored fruit leathers (figure 3.2.3). However, a significant decrease of degradation speed was observed in the real sample solution/suspension vs. the simpler model system (table 3.2.1). The suspended pulp ingredients and other ingredient background from the fruit leather products could reduce ozonation efficiency, either via physical or chemical means. According to the *L* value obtained with the Hunter colorimeter, an increased lightness was observed against ozone dose increase (figure 3.2.4), which resulted from removal of total colorant amount. Unlike results from the UV/Vis measurement, the Hunter colorimeter readings did not indicate a specific degradation pattern of

colorants. The random curves obtained from the Hunter colorimeter might be the result of mixed colorants and differences in their degradation kinetics.

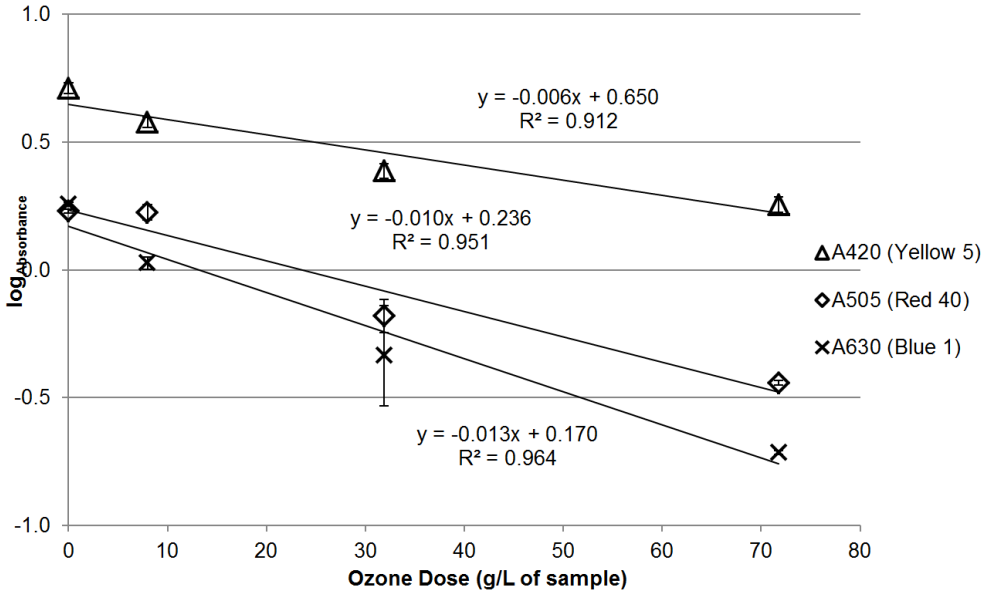

Figure 3.2.3. Efficiency of ozone decolorization for colorants present in fruit leather solution/suspension. Ozone at 26.6 mg/L·min was introduced into a 200 mL 100% fruit leather solution/suspension sample with 800 mL/min air flow.

Table 3.2.1. Decolorization efficiencies of Yellow 5, Red 40 and Blue 1.

Sample	Colorant	Equation	R^2	Average RSD/%
Colorant aqueous solution	Yellow 5	$\log A = -4.953 \cdot D_{ozone} + 0.848$	0.983	3.47
	Red 40	$\log A = -9.407 \cdot D_{ozone} + 1.010$	0.944	22.7
	Blue 1	$\log A = -22.33 \cdot D_{ozone} + 0.769$	0.986	6.41
100% Fruit leather solution/suspension	Yellow 5	$\log A = -0.006 \cdot D_{ozone} + 0.650$	0.912	6.39
	Red 40	$\log A = -0.010 \cdot D_{ozone} + 0.236$	0.951	13.6
	Blue 1	$\log A = -0.013 \cdot D_{ozone} + 0.170$	0.964	38.7

Note: In the equation, D_{ozone} is ozone dose, and in g/L of sample, and A is the light absorbance of the colorant at its maximum absorptivity wavelength.

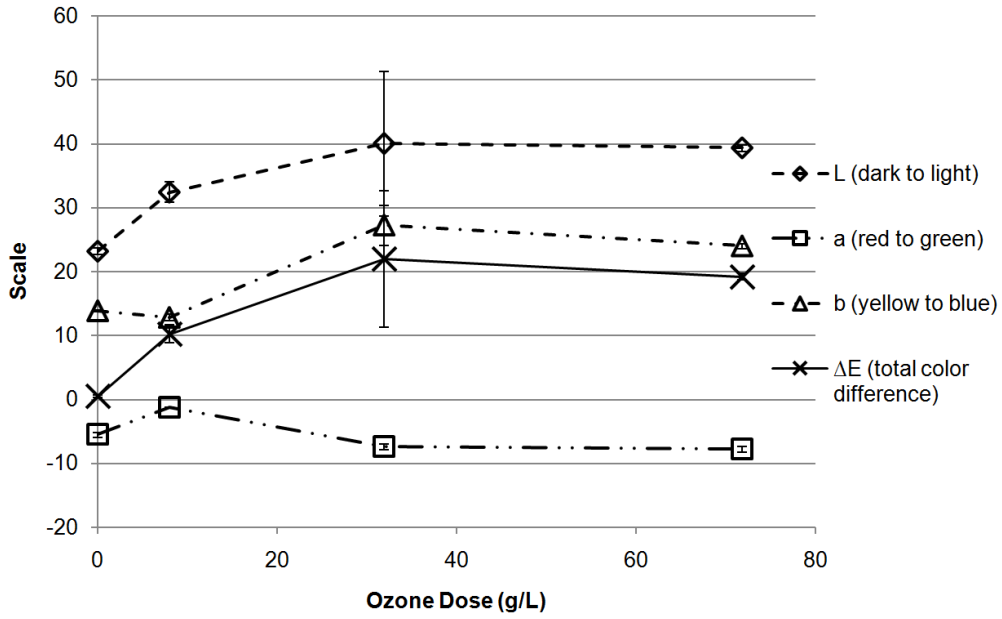

Figure 3.2.4. Hunter colorimeter measurements.

3.3. Byproduct Screening

According to previous studies, the N=N and C-N bonds are subject to oxidation, and tend to break down (Gosseti et al., 2005, 2007 and 2008; Ozsoy et al., 2008b). Natural light, or ambient nitric acid and ambient ozone were found to be oxidative enough to degrade colorants into smaller molecules (Gosseti et al., 2005, 2007 and 2008; Grosjean et al., 1988 and 1992). However, carbonyl compounds were not identified as colorant degradation products in previous studies.

In this study, ozonated samples were submitted to SPME-GC-MS analysis to identify byproducts, and to determine the target compounds to monitor. Carbonyl compounds were identified as major byproducts (table 3.3.1). For a more thorough identification of carbonyls, derivatization SPME with PFBHA was performed. Generation of chemicals with low molecular weight in this study might be caused by high oxidative potential of ozone at high concentration when introduced into the sample solution.

No nitrogen-containing products were detected, which could result from mineralization of these colorants. These results agree with an earlier study on ozone treatment of Acid Orange 6 (Hsing et al., 2007). The high oxidation potential of ozone is expected to induce open-ring and mineralization reactions. The detection of carbonyl compounds as major products suggests ring-opening reaction mechanisms. Regarding carbonyl compounds analysis, on-fiber derivatization SPME was compared with a SPME method without derivatization. We found that a considerable enhancement of selectivity and sensitivity of SPME was achieved through use of on-fiber derivatization (Figure 3.3.1). The method was selected in the following study to quantify carbonyl compounds as major and potentially toxic byproducts.

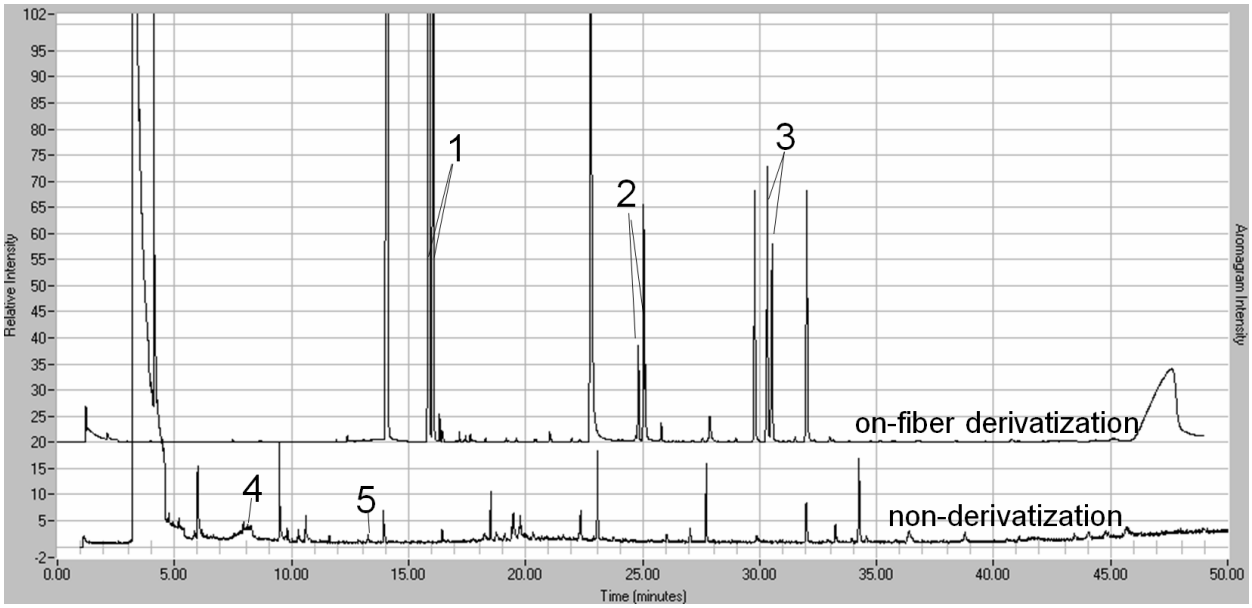

Figure 3.3.1. Comparison of on-fiber derivatization SPME and non-derivatization SPME. 1. *trans/cis* ethanal-PFBHA oxime; 2. *trans/cis* hexanal-PFBHA oxime; 3. *trans/cis* octanal-PFBHA oxime; 4. hexanal; 5. octanal.

Table 3.3.1. Byproduct chemicals identified in ozonated colorant aqueous solutions.

Compound	LD_{50}-rat-oral (mg/kg) [b]	Detected or not			
		Blue	Red	Yellow	Green
Ethanal	661	Yes	Yes	Yes	Yes
Propanal	1,600	Yes	Yes	Yes	Yes
Butanal	5,890	Yes	Yes	Yes	Yes
Pentanal	4,581	Yes	Yes	Yes	Yes
Hexanal	4,890	Yes	Yes	Yes	Yes
Heptanal	14,000	Yes	Yes	Yes	Yes
Octanal	5,630	Yes	Yes	Yes	Yes
Nonanal	5,000	Yes	Yes	Yes	Yes
Decanal	23,000	Yes	Yes	Yes	Yes
Acetone	5,800	Yes	Yes	Yes	Yes
Butanone	2,737	Yes	Yes	Yes	Yes
2-Pentanone	1,600	Yes	Yes	Yes	Yes
2-Heptanone	1,670	Yes	Yes	Yes	Yes
6-Methyl-2-heptanone	N/A	No	Yes	Yes	No
Furfural	65	Yes	Yes	Yes	Yes
Benzaldehyde	1,300	Yes	Yes	Yes	Yes
Furan	300	Yes	Yes	Yes	Yes
Acetic acid	3,310	Yes	Yes	Yes	Yes

Table. 3.3.1. continued.

2-Butenoic acid	400	No	No	Yes	No
Benzoic acid[a]	1,700	Yes	Yes	Yes	Yes
2-Ethyl-1-hexanol	3,730	Yes	Yes	Yes	Yes
1-Dodecanol	1,800	Yes	Yes	Yes	No
Furfuryl alcohol[a]	177	Yes	Yes	Yes	Yes
Phenol[a]	410	Yes	Yes	Yes	Yes
1-Tetradecanol	5,000	No	Yes	Yes	No
Tetradecanol	5,000	No	No	Yes	No
Ethoxy-1-dodecanol	N/A	No	No	Yes	No
Diethyl phthalate	8,600	No	Yes	Yes	No

Note: Chemicals were identified in the chromatograms generated from DI-SPME-GC-MS, and on-fiber derivatization SPME-GC-MS analysis.

[a] The chemical was also identified in the untreated commercial food colorant aqueous solution.

[b] The LD_{50} values were acquired from Material Safety Data Sheets.

3.4. Development of On-fiber Derivatization SPME-GC-MS Method

In the process of on-fiber derivatization, the actual extraction phase is the derivatization reagent doped onto the SPME fiber. Mass transport of the chemicals from the liquid phase to the headspace, and the kinetics of the derivatization reaction both influence the uptake of carbonyls. Derivatization-time profiles of on-fiber derivatization were generated based on different PFBHA doping concentrations (0.5, 3.75 and 17 mg/mL). The concentration of each carbonyl compound in the standard solution was about 5 ng/mL. An increase of equilibrium time was observed with

increased PFBHA doping concentration. Equilibrium times were 15, 30 and 60 min, respectively, with PFBHA solution at 0.5, 3.75 and 17 mg/mL. Within the equilibrium time, no obvious variation of the uptake rate for carbonyls was observed. However, longer equilibrium time allows higher recovery with longer extraction time (figure 3.4.2). To achieve higher uptake rate, the highest dopant solution concentration at 17 mg/mL was selected. Doping time of PFBHA onto the fiber was 15 min.

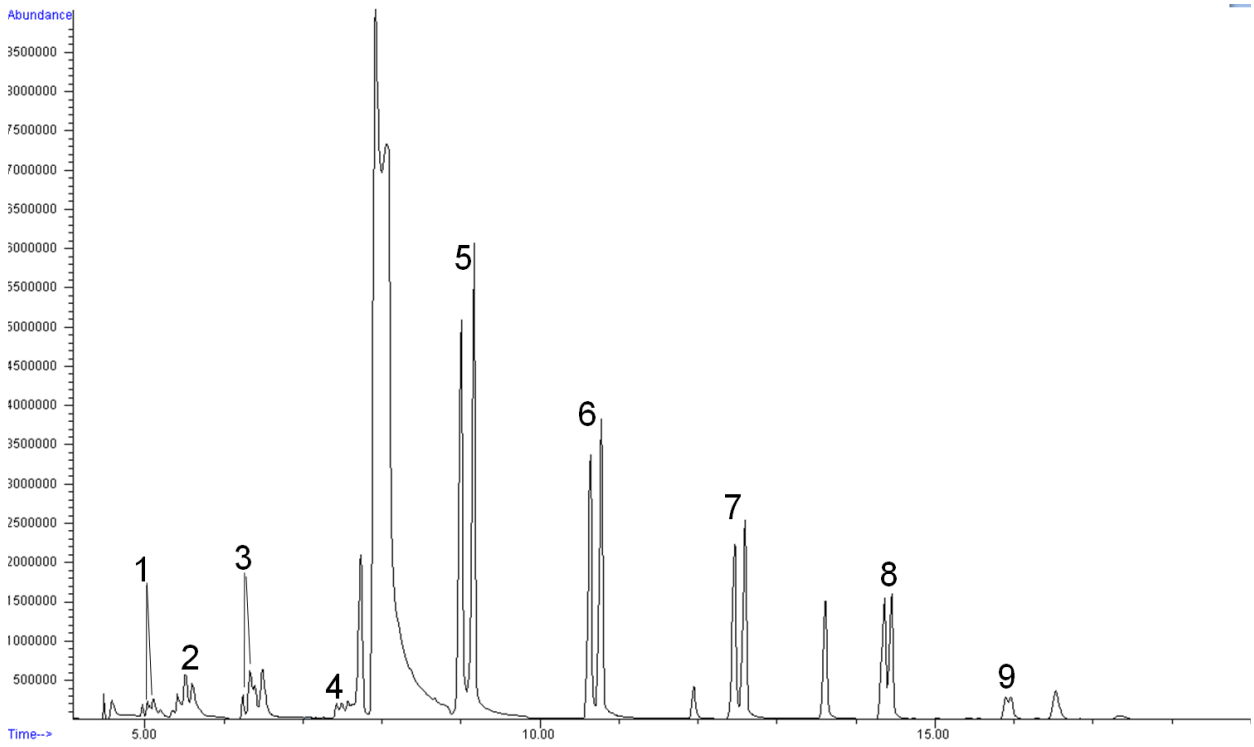

Figure 3.4.1. Chromatogram of on-fiber derivatization SPME of ozonated fruit leather solution/suspension. 1. Ethanal, 2. Propanal, 3. Butanal, 4. Pentanal, 5. Hexanal, 6. Heptanal, 7. Octanal, 8. Nonanal, 9. Decanal.

Note: Two isomeric oximes (*trans/cis*) were formed for each aldehyde (except for acetone with a symmetric structure). Peak areas of both isomers were summed up for quantification.

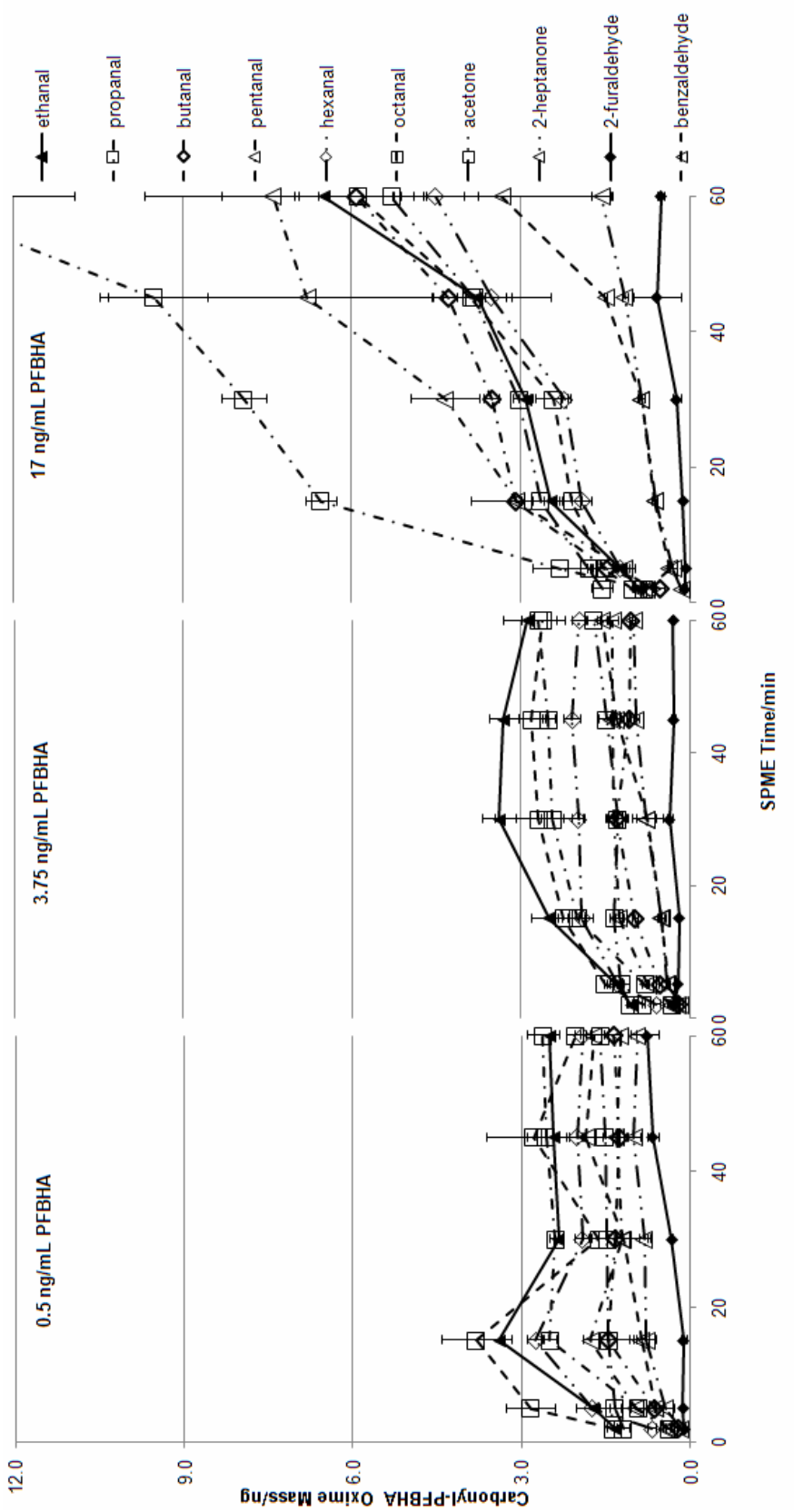

Figure 3.4.2. Comparison of different PFBHA doping concentrations according to the derivatization-time profiles.

Table 3.4.1. Validation of on-fiber derivatization with 17 mg/mL PFBHA

Chemical	log P_{ow}	Response Factor (peak area count/mass (ng))	Extraction-time Linearity (R^2)		Average RSD (%)		
			5 – 60 min	2 – 20 s	5 – 60 min	2 – 20 s	5 s
Ethanal	0.63	86,606	0.932	0.932	12.7	10.2	14.4
Propanal	0.83	60,185	0.942	ND	13.7	ND	ND
Butanal	0.88	341,983	0.930	0.969	11.1	8.94	10.4
Pentanal	-0.16	73.405	0.973	ND	24.6	ND	ND
Hexanal	2.33	64,194	0.973	0.957	12.3	15.9	7.90
Octanal	3.03	31,414	0.941	0.930	10.5	24.4	17.7
Acetone	-0.24	112,134	0.968	0.562	8.64	8.43	4.19
2-Heptanone	1.98	125,294	0.988	0.825	10.8	25.0	17.3
2-Furfural	0.41	100,814	0.874	0.963 [a]	29.1	14.3	1.61
Benzaldehyde	1.48	130,920	0.776	0.999 [a]	17.1	14.4	9.34

Note: Response factor = peak area count/carbonyl injection mass (ng). ND: not detected.

[a] Linearity was calculated within 2 – 10 s of extraction.

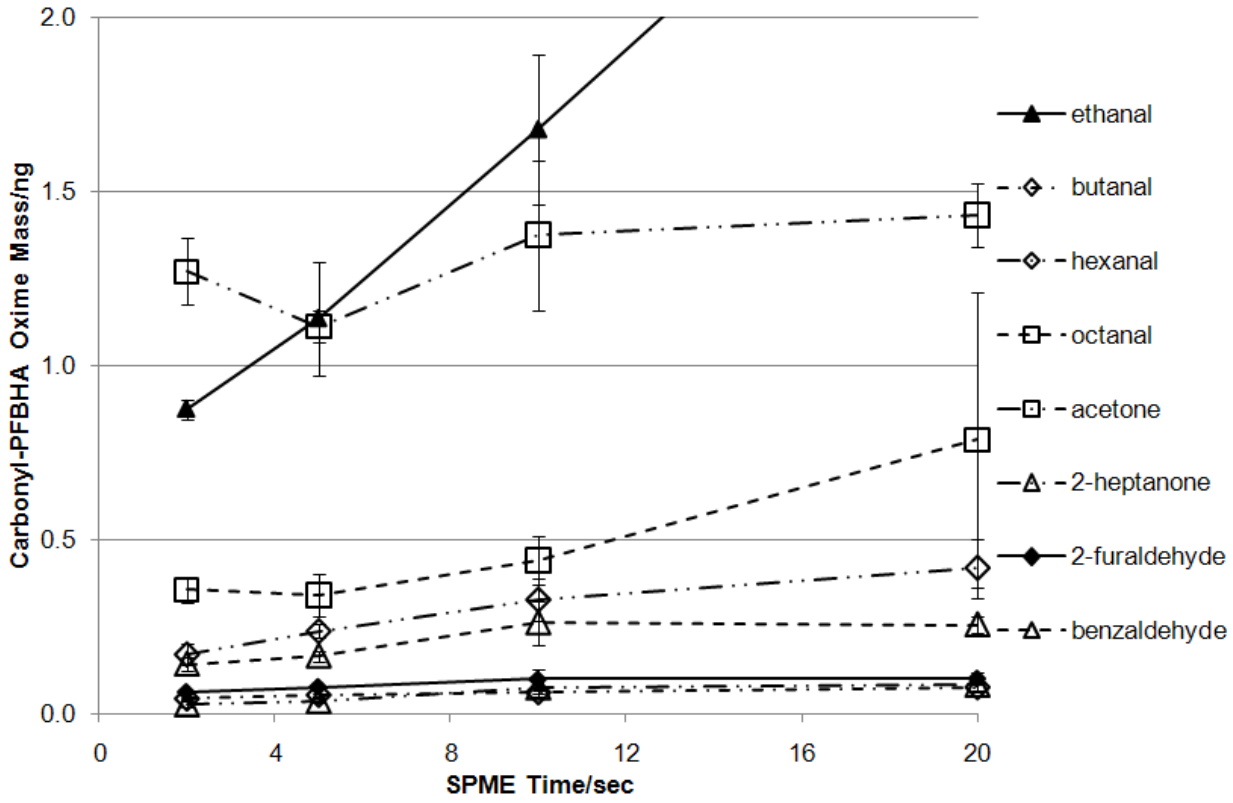

Figure 3.4.3. Time-profile of derivatization time from 2 – 20 s.

With PFBHA at 17 mg/mL, extraction of aliphatic aldehydes (ethanal, propanal, butanal, pentanal, hexanal, and octanal), and aliphatic ketones (acetone, and heptanone) increased linearly against time with $R^2 > 0.93$. An exception was observed with 2-furfural, whose derivative decreased within 5 min derivatization. The log P_{ow} value of 2-furfural suggests a medium diffusion effect among other carbonyls (table 3.4.1). It is expected that the displacement resulted from higher reaction kinetics of other competing carbonyls. Shorter on-fiber derivatization time was tested. The concentration of ethanal was about 2 µg/mL, while each other chemical was at about 5 ng/mL. The displacement of 2-furfural was avoided within 10 s derivatization – long before the equilibrium or saturation. The prevention of the displacement of 2-furfural

significantly decreased inaccuracy from average RSD = 29.1% to 14.3%. Five seconds was used for on-fiber derivatization with RSD = 1.61%. Recovery decreased with a shorter derivatization time (figure 3.4.2 and 3.4.3), while the accuracies on 2-furfural and benzaldehyde were enhanced.

Figure 3.4.5 and 3.4.6 show the effects of temperature on the uptake efficiency of carbonyls. The fiber was doped with 17 mg/mL PFBHA at the same temperature, 40, 60 or 80 ˚C, as in the derivatization procedure. The concentration of each carbonyl compound in the standard solution was about 5 ng/mL for the 30min extraction test. For the 10 s extraction test, ethanal was at 2 µg/mL, while other chemicals were at 5 ng/mL. Highest recovery of most compounds was obtained at 60 ˚C. In the study to follow, PFBHA doping and on-fiber derivatization were performed at 60 ˚C.

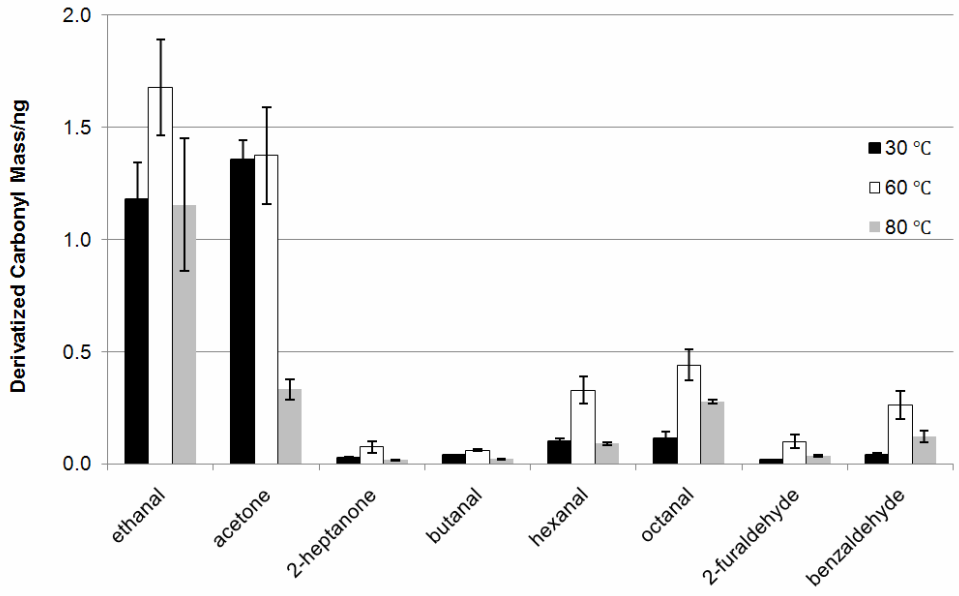

Figure 3.4.5. Effects of temperature on 10 s on-fiber derivatization efficiency

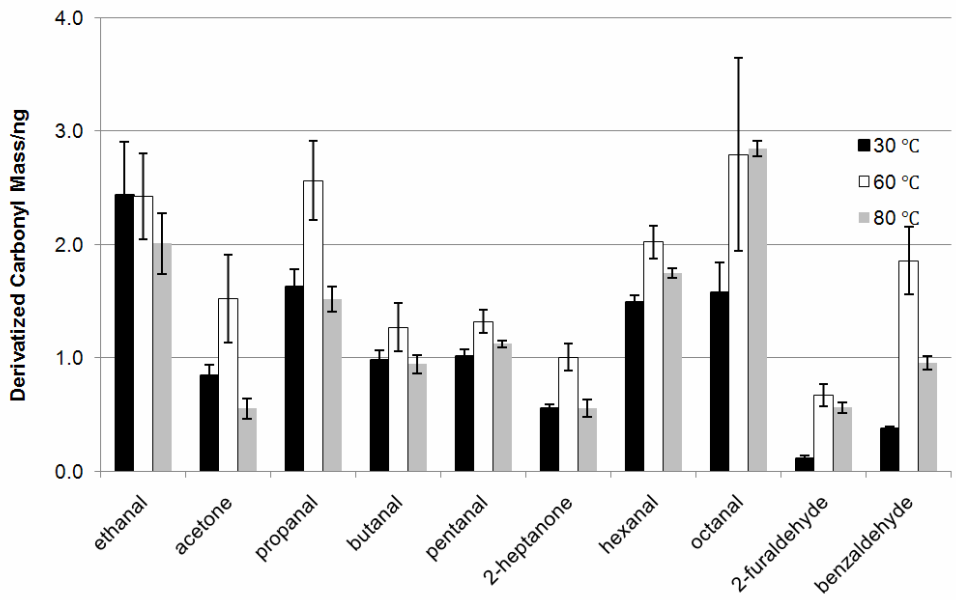

Figure 3.4.6. Effects of temperature on 30 min on-fiber derivatization efficiency

Optimum analysis conditions were established to be: PFBHA dopant concentration at 17 mg/mL, doping time for 15 min, derivatization time for 10 s, and doping and derivatization temperature at 60℃. Based on the developed extraction method, quality parameters such as linearity, detection limit, and precision were determined (Table 3.4.2). Calibration curves of ethanal, hexanal, 2-furfural and benzaldehyde were generated by plotting quantification ion peak areas against the corresponding carbonyl compound concentration in the standard sample.

Three options are typically available to perform derivatization with SPME: derivatization in GC injection port, direct derivatization in sample matrix and derivatization in SPME fiber coating. Derivatization in the GC injector calls for injection of derivatization reagent in the injector before thermal desorption of SPME fiber, and derivatization was the sampling procedure afterwards. In this study, SPME failed to uptake ethanal before derivatization, and this method was not considered. With direct derivatization in a sample matrix, higher sensitivity was usually

reported in previous studies on aldehyde analysis (table 3.4.3). However, longer derivatization times - up to several hours, were needed in a diluted system. On-fiber derivatization SPME was proven to be a rapid sampling method for carbonyl compounds in this study. Sensitivity at ppb levels was achieved with a very short derivatization time (table 3.4.2), compared with direct derivatization.

Table 3.4.2. Linearity and sensitivity of the new on-fiber derivatization SPME-GC-MS method.

Compound	**Calibration Curve**	**R^2**	**LOD (µg/L)**
Ethanal	$y = 1.2\times10^{3}x + 70324$	0.9831	0.030
Hexanal	$y = 9.2\times10^{2}x + 29024$	0.9959	0.029
2-Furfural	$y = 3.7\times10^{4}x + 35313$	0.9579	0.016
Benzaldehyde	$y = 4.1\times10^{4}x + 38523$	0.9874	0.016

Table 3.4.3. Studies of carbonyl compounds derivatization with SPME.

Study	Matrix	Analysis Method	Derivatization Method	Chemical	LOD/ ppb(v)
Bao et al., 1998	Water	SPME-GC/ECD	Direct derivatization-liquid SPME	Formaldehyde	0.015
				Ethanal	0.02
				Hexanal	0.035
				Benzaldehyde	0.008
				Aldehydes, dialdehydes and ketones	0.006–0.2
			Direct derivatization-head space-SPME	Formaldehyde	0.02
				Ethanal	0.03
				Hexanal	0.025
				Benzaldehyde	0.990
				Aldehydes, dialdehydes and ketones	0.006–0.2

Table. 3.4.3. continued.

Beránek et al. 2008	Water	SPME-GC-MS	Direct derivatization-head space-SPME	Formaldehyde	108
				2-Furfural	1.6
				Ethanal	11
				Benzaldehyde	0.5
				Hexanal	0.7
				Alkanals, alkenals, dialdehydes and phenyl aldehydes, etc.	0.5–53
			Direct derivatization-liquid SPME	Formaldehyde	55
				Ethanal	1.0
				Hexanal	0.5
				Benzaldehyde	0.6
				2-Furfural	0.5
				Alkanals, alkenals, dialdehydes and phenyl aldehydes, etc.	0.1–4.4
			On-fiber derivatization	Formaldehyde	53
				Ethanal	3.7
				Benzaldehyde	2.3
				2-Furfural	35
				Hexanal	0.7
				Alkanals, alkenals, dialdehydes and phenyl aldehydes, etc.	0.1–55

Table. 3.4.3. continued.

Saison et al., 20090	Beer	SPME-GC-MS	Direct derivatization-head space-SPME	Hexanal	0.010
				Benzaldehyde	0.010
				2-Furfural	0.66
				Alkanals, alkenals, ketones, phenyl aldehydes, furan derivatives and dicarbonyls, etc.	0.003–310
			On-fiber derivatization	Hexanal	0.028
				Benzaldehyde	0.078
				2-Furfural	6.0
				Alkanals, alkenals, ketones, phenyl aldehydes, furan derivatives and dicarbonyls, etc.	0.004–20,000
Bianchi et al., 2007	Fish	SPME-GC-MS	On-fiber derivatization	Formaldehyde	17
Deng et al., 2004	Human blood	SPME-GC-MS	On-fiber derivatization	Ethanal	0.44×10^{-4}
				Hexanal	6.0×10^{-4}
				Alkanals	0.44×10^{-4}–6.0×10^{-4}
Iglesias et al., 2010	Fish	SPME-GC-MS	On-fiber derivatization	Ethanal	1.6
				Hexanal	1.6
				Alkanals, alkenals, dialkenals, furfural and benzaldehyde, etc.	0.42–1.8
Koziel et al., 2007	Ambient air	SPME-GC-MS	On-fiber derivatization	Formaldehyde	1.0

Table. 3.4.3. continued.

Martos et al., 1998	Ambient air	SPME-GC-MS	On-fiber derivatization	Formaldehyde	4.6
Stashenko et al., 2006	Air	SPME-GC/ECD	On-fiber derivatization	Ethanal	6.06×10^{-5}
				Hexanal	3.84×10^{-5}
				Alkanals	0.59×10^{-5}–4.59×10^{-5}
Trenholm et al., 2008	wastewater	SPME-GC-MS	On-fiber derivatization	Formaldehyde	3.7
Tsai et al., 2003	Water	SPME-GC-MS	On-fiber derivatization	Formaldehyde	0.22
				Alkanals	0.12–0.34
Schmarr et al., 2008	Alcohol and grape seed oil	2D-GC-MS	On-fiber derivatization	Alkanals, (E)-2-alkenals, and (E,E)-2,4-alkadienals	N/A
This study	Ozonated water	SPME-GC-MS	On-fiber derivatization	Ethanal	0.030
				Hexanal	0.029
				Benzaldehyde	0.016
				2-Furfural	0.016
Lin et al., 2008	Tobacco smoke	GC-μFID	Direct derivatization-head space-SPME	Ethanal	47740
Cancho et al., 2001	Water	SPME-GC-MS	Direct derivatization-head space-SPME	Ethanal	0.04
				Alkanals and dialdehydes	0.04–0.4

Table. 3.4.3. continued.

Le Lacheur et al., 1993	Ozonated paper pulp and water	Smog chamber-GC-MS	Direct derivatization-LLE	Alkanals, dialdehydes, ketones and unsaturated ketones, etc.	N/A
Culleré et al., 2004	Wine	SPE-GC-MS	PFBHA imbedded in SPE cartridge	3-Methylbutanal, E-2-hexenal, E-2-heptenal, E-2-octenal and phenylacetaldehyde	0.12–0.70
Ortiz et al., 2006	Atmospheric air	GC-MS	PFBHA coated annular denuder	Glyoxal, methylglyoxal, glycolaldehyde and hydroxyacetone	N/A
Pang et al., 2008	Engine exhaust	HPLC-DAD-MS	DNPH-coated silica gel cartridges	Alkanals, acrolein, acetone, and phenyl aldehydes, etc.	N/A
Tsai et al., 2006	Atmospheric air	Diffusive sampler-SPME-GC-MS	On-fiber derivatization	2-Furfural	N/A

3.5. Real Sample Analysis

Based on the on-fiber derivatization-SPME-GC-MS analysis results, a carbonyl generation-dose of ozone profile was obtained. Generation of all carbonyls reached at a peak value at the same ozone dosage. A decrease was observed following the highest generation, to which either vaporization or oxidation of carbonyl compounds, or both could be contributive. The increase in aliphatic acids suggest oxidation was also a contributing factor (figure 3.5.2). The maximum generation is listed in table 3.5.1.

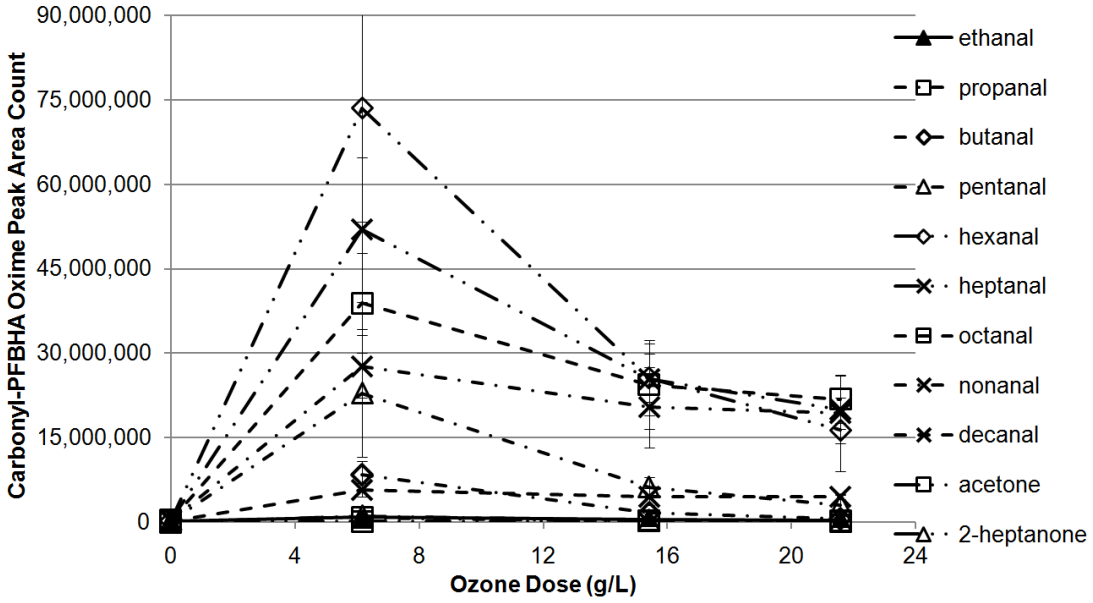

Figure 3.5.1. Carbonyl generation-ozone dose profile. Ozone was introduced at a rate of 26.6 $mg/L \cdot min^{-1}$ into a 200 mL 100% fruit leather solution/suspension. The sample was submitted to on-fiber derivatization SPME-GC-MS analysis.

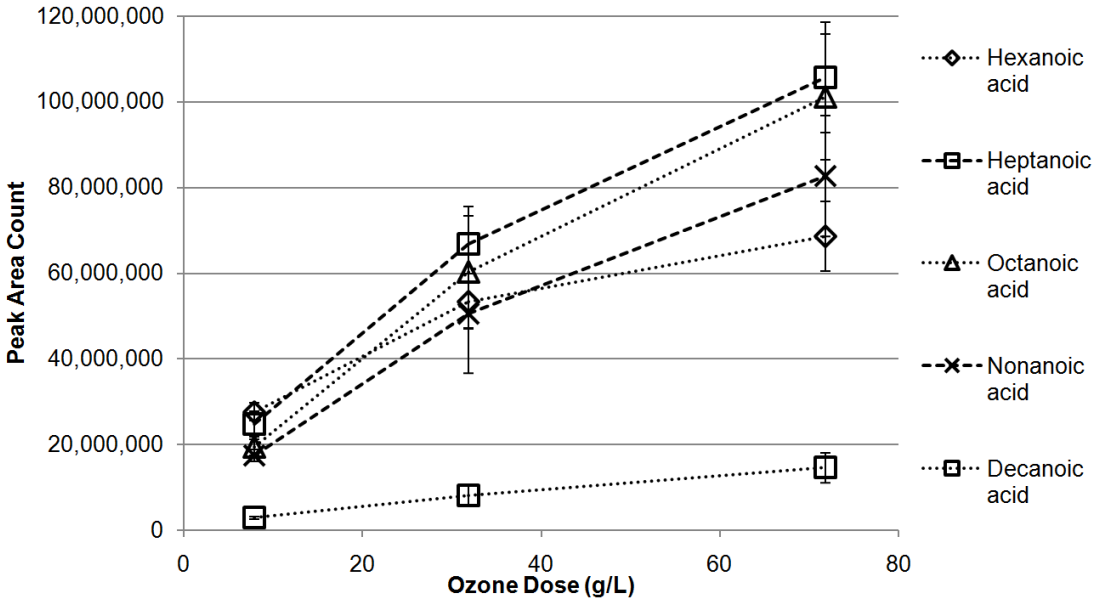

Figure 3.5.2. Aliphatic acid generation-ozone dose profile. Ozone at 26.6 mg/L·min^{-1} was introduced into a 200 mL 100% fruit leather solution/suspension. The sample was submitted to HS-SPME-GC-MS analysis.

Because the intent of our work was to safely decolorize out of specification fruit leather so that it could be recycled and reworked back into salable product, a primary risk assessment of the major carbonyl byproducts of fruit leather ozonation was performed (table 3.5.1). Our serving of commercial product weights ~10 g) of fruit leather every day in average and that 1 kg fruit leather can be recycled from 1 L of decolorized 100% fruit leather solution/suspension. Next, by taking the highest level generated (C_{max}) for each chemical as its concentration in recycled solution/suspension, we calculate that for ozone-recycled fruit leather, the concentration (C_{fl}) equals to C_{max}/(1 kg of fruit leather/L of solution/suspension). Therefore, an adult weighing 70 kg (154 lbs), consuming 10 g fruit leather each day would have an intake of 10 g × C_{fl}/70 kg body weight per day of byproduct chemical. Calculated intake results for each major carbonyl

compound are shown in table 3.5.1. These results show that intake of these compounds is below the Oral Reference Dose (RfD) value, an estimate of daily exposure that doesn't result in appreciable risk to humans during a lifetime. The rest of the byproducts are of very low concentration. According the Hodge and Sterner Scale (Chen et al., 2006), these chemicals are practically non-toxic. Moreover, it is worth of noticing that some carbonyl compounds are important in fruit flavors, such as ethanal, octanal and decanal were found contributive to citrus flavors (Fennema et al., 1996).

Table 3.5.1. Quantification results of major carbonyl byproducts of concern.

Compound	**Calibration Curve**	**LOD (µg/L)**	**C_{max} (mg/L)**	**Intake (mg/kg·day^{-1})**	**Oral RfD (mg/kg·day^{-1})**
Ethanal	$y = 1.2\times10^{3}x + 70324$	0.030	0.644 ± 0.188	$(9.2 \pm 2.7) \times 10^{-5}$	0.04[a]
Hexanal	$y = 9.2\times10^{2}x + 29024$	0.029	80.0 ± 22.0	0.011 ± 0.003	
2-Furaldehyde*	$y = 3.7\times10^{4}x + 35313$	0.016	$< 1.6 \times 10^{-5}$	$< 2.29 \times 10^{-9}$	
Benzaldehyde	$y = 4.1\times10^{4}x + 38523$	. 0.016	$< 1.6 \times 10^{-5}$	$< 2.29 \times 10^{-9}$	0.1[b]

Note: Conservative assumptions were made to estimate intake values.

[a] Til et al., 1988

[b] Kluwe et al., 1983

* 5-nitro-,4-(3-(diethylamino)propyl)semicarbazone,

or 5-Nitro-2-furaldehyde 4-(3-(diethylamino)propyl)semicarbazone

or 1-(5-Nitro-2-furfurylidine)-3-N,N-diethylpropylaminourea hydrochloride

3.6. Cost and Profit Estimation

Major costs for this recycling system include installation of transportation pathways, storage and treatment containers, electricity and labor for equipment operation, and facility maintenance. The initial installation is expected to cost $100k – 150k, or $15k – 22k per year over ten years of usage. The maintenance of such a system costs $4k – 6k per year (Ozsoy et al., 2008b). For 100% fruit leather solution/suspension, sufficient color removal in laboratory scale requires 70 g ozone/L solution. This equals 70 g ozone/1,000 g fruit leather. Therefore, recycling of 1,000 tons fruit leather per year would require 140 tons ozone. Cost per unit of ozone is estimated to be $0.09/kWh × 12 kWh/kg ozone (Ozsoy et al., 2008b), or about $150 per ton. Other complementary systems such as transportation and drying are expected to add $50 per ton, with a total operational expense of $200/ton. The estimates above transfer to a $50K – 60K of capital investment per year, or $50 – $60 per ton of fruit leather. With an estimated value of recycled fruit leather of $500/ton and if 1,000 tons are recycled annually, this process could potentially result in a $0.25 million profit per year, not including the savings on costs associated with traditional methods for waste fruit leather disposal.

Chapter 4. Conclusions

An ozone-based decolorization method was proven to be an effective, additive-free approach for removing colorants in fruit leather products. With selectivity based on the absorptivity of different colorants, UV/Vis spectrometry was proven to be an appropriate technique in the measurement of mixed colorants. The measurement results demonstrated that colorant degradation in this system was pseudo-first order.

Mineralization and ring-opening reactions were observed in the ozone decomposition of food colorants Blue 1, Red 40 and Yellow 5. Carbonyl compounds were identified as major byproducts from the decomposition. On-fiber derivatization SPME coupled with GC-MS was proven to be an ideal analytical method for the quantification of byproducts with high concern in this case study. The LOD values of the developed method were in the range of 0.016 to 0.030 ppb; linearity for 2-furfural was the lowest with $R^2 = 0.9579$ in the range of 0.04 – 0.8 ng/L; hexanal was analyzed in a linear range of 20 – 8000 ng/L, with the highest $R^2 = 0.9959$. The high sensitivity of on-fiber derivatization SPME also allows application in carbonyl compound analysis in different situations. Waste fruit leather before and after ozone-based decolorization process was analyzed for the determination of carbonyl content. Benzaldehyde and 2-furfural were generated below LOD, 0.016 μg/L of 100% fruit leather solution/suspension, while hexanal was the most abundantly generated, and the maximum generation was 80.0 ± 22.0 mg/L. A conservative risk assessment was performed based on quantification results and toxicity information of the chemicals, the results of which suggest the acceptability of ozone-based decolorization in fruit leather recycling from a safety standpoint. The cost for installation and operation of ozone-based decolorization equipment was estimated against the value of

recycled/reclaimed materials, and an annual profit of $0.25 million is expected, not including savings from traditional costs associated with disposal of product.

Acknowledgements

I would like to express my most sincere gratitude to my advisors Dr. Jacek Koziel and Dr. Hans van Leeuwen as my major professors for their great support in many aspects in my graduate study and research. I appreciate their patient and wise guidance which always encouraged me to think of correct approaches.

I want to thank Dr. Lingshuang Cai for her supervision on my first year research, and kind-hearted help during my master's study. My sincere thanks also go to Dr. Byron Brehm-Stecher, my other committee member, offering much attention and advice to my research project.

I appreciate this opportunity to study at Iowa State University. This experience is a precious fortune in my life.

References

Aksu, Z.; Karabayir, G. Comparison of biosorption properties of different kinds of fungi for the removal of Gryfalan Black RL metal-complex dye *Bioresource Technology* **2008**, 99, 7730–7741

Ao, C.H.; Leung, M.K.H.; Lam, R.C.W.; Leung, D.Y.C.; Vrijmoed, L.L.P.; Yam, W.C.; Ng, S.P. Photocatalytic decolorization of anthraquinonic dye by TiO_2 thin film under UVA and visible-light irradiation *Chemical Engineering Journal* **2007**, 129, 153–159

Bao, M.; Pantani, F.; Griffini, O.; Burrini, D.; Santianni, D.; Barbieri, K. Determination of carbonyl compounds in water by derivatization-solid-phase microextraction and gas chromatographic analysis *Journal of Chromatography A* **1998**, 809, 75–87

Beránek, J.; Kubatova, A. Evaluation of solid-phase microextraction methods for determination of trace concentration aldehydes in aqueous solution *Journal of Chromatography A* **2008**, 1209, 44–54

Bianchi, F.; Careri, M.; Musci, M.; Mangia, A. Fish and food safety: Determination of formaldehyde in 12 fish species by SPME extraction and GC–MS analysis *Food Chemistry* **2007**, 100, 1049–1053

Cancho, B.; Ventura, F.; Galceran, M.T. Determination of aldehydes in drinking water using pentafluorobenzylhydroxylamine derivatization and solid-phase microextraction *Journal of Chromatography A* **2002**, 943, 1–13

Chaw, Y.M.; Crane, L.E.; Lange P. and Shapiro, R. Isolation and identification of cross-links from formaldehyde treated nucleic acid *Biochemistry* **1980**, 19, 5525–5531

Chen, X.; Qiao, X.; Wang, D.; Lin, J.; Chen, J. Kinetics of oxidative decolorization and mineralization of Acid Orange 7 by dark and photoassisted Co^{2+}-catalyzed peroxymonosulfate system *Chemosphere* **2007**, 67, 802–808

Chen, Z.; Meng, H.; Xing, G.; Chen, C.; Zhao, Y.; Jia, G.; Wang, T.; Yuan, H.; Ye, C.; Zhao, F.; Chai, Z.; Zhu, C.; Fang, X.; Ma, B. and Wan, L. Acute toxicological effects of copper nanoparticles in vivo *Toxicology Letters* **2006**, 163, 109-120

Chi, Y.; Feng, Y.; Wen, S.; Lu, H.; Yu, Z.; Zhang, W.; Sheng, G.; Fu, J. Determination of carbonyl compounds in the atmosphere by DNPH derivatization and LC–ESI-MS/MS detection *Talanta* **2007**, 72, 539–545.

Chutintrasri, B.; Noomhorm, A. Color degradation kinetics of pineapple puree during thermal processing *LWT* **2007**, 40, 300–306

Chu, L.; Xing, X.; Yu, A.; Zhou, Y.; Sun, X. and Jurcik, B. Enhanced ozonation of simulated dyestuff wastewater by microbubbles *Chemosphere* **2007**, 68, 1854–1860

Clesceri, L.S.; Greenberg, A.E.; Eaton, A.D. Ozone demand/requirement semi-batch method, part 2350E in Standard methods for the examination of water and wastewater, American Public Health Assoc., American Water Works Assoc. and Water Environment Federation, ISBN: 0-87553-235-7, **1998**

Colombini, M.P.; Andreotti, A.; Baraldi, C.; Degano, I.; Łucejko, J.J. Colour fading in textiles: A model study on the decomposition of natural dyes *Microchemical Journal* **2007**, 85, 174–182

Culleré, L.; Cacho, J.; Ferreira, V. Analysis for wine C5–C8 aldehydes through the determination of their O-(2,3,4,5,6-pentafluorobenzyl)oximes formed directly in the solid phase extraction cartridge *Analytica Chimica Acta* **2004**, 524, 201–206

Deng, C. and Zhang, X. A simple, rapid and sensitive method for determination of aldehydes in human blood by gas chromatography/mass spectrometry and solid-phase microextraction with on-fiber derivatization *Rapid Commun. Mass Spectrom.* **2004**, 18, 1715–1720

Feldman, V.J. and Kruysse, A. Effects of exposure to acrolein vapor in hamsters simultaneously treated with benzo[α]pyrene or diethylnitrosamine *J. Toxicol. Environ. Health* **1978**, 3, 379–394

Fennema, O.R. Food Chemistry, CRC Press, ISBN: 0-8247-9346-3, **1996**

Flamini, R.; Vedova, A.D.; Panighel, A.; Perchiazzi, N. and Ongarato, S. Monitoring of the principal carbonyl compounds involved in malolactic fermentation of wine by solid-phase microextraction and positive ion chemical ionization GC/MS analysis *J. Mass Spectrom.* **2005**, 40, 1558–1564

Forgacs, E.; Cserhati, T.; Oros, G. Removal of synthetic dyes from wastewaters: a review *Environmental International Epigallocatechin*, 30, 953–971

Fu, Y.; Viraraghavan, T. Fungal decolorization of dye wastewaters: a review *Bioresource Technology* **2001**, 79, 251–262

Ghodbane, H.; Hamdaoui, O. Intensification of sonochemical decolorization of anthraquinonic dye Acid Blue 25 using carbon tetrachloride *Ultrasonics Sonochemistry* **2009**, 16, 455–461

Glaze, W.H.; Peyton, G.R.; Lin, S.; Huang, R.Y. and Burieson, J.L. Destruction of Pollutants in Water with Ozone in Combination with Ultraviolet Radiation. 2. Natural Trihalomethane Precursors *Envlron. Scl. Technol.* **1982**, 16, 454–458

Gosetti, F.; Gianotti, V.; Polati, S.; Gennaro, M.C. HPLC-MS degradation study of E110 Sunset Yellow FCF in a commercial beverage *Journal of Chromatography A* **2005**, 1090, 107–115

Gosetti, F.; Frascarolo, P.; Mazzucco, E.; Gianotti, V.; Bottaro, M.; Gennaro, M.C. Photodegradation of E110 and E122 dyes in a commercial aperitif A high performance liquid chromatography–diode array–tandem mass spectrometry study *Journal of Chromatography A* **2008**, 1202, 58–63

Gosetti, F.; Gianotti, V.; Angioi, S.; Polati, S.; Marengo, E.; Gennaro, M.C. Oxidative degradation of food dye E133 Brilliant Blue FCF Liquid chromatography–electrospray mass spectrometry identification of the degradation pathway *Journal of Chromatography A* **2004**, 1054, 379–387

Gosetti, F.; Gianotti, V.; Mazzucco, E.; Polati, S.; Gennaro, M.C. Sunlight induced degradation of E133 in a commercial beverage *Dyes and Pigments* **2007**, 74, 424–432

Grosjean, D.; Salmon, L.G. and Cas, G.R. Fading of Organic Artists' Colorants by Atmospheric Nitric Acid: Reaction Products and Mechanisms *Environ. Sci. Technol.* **1992**, 26, 952–959

Grosjean, D.; Whitmore, P.M.; De Moor, C.P. and Cass, G.R. Ozone Fading of Organic Colorants: Products and Mechanism of the Reaction of Ozone with Curcumin *Environ. Sci. Technol.* **1988**, 22, 1357–1361

Guzel-Seydim, Z.B.; Greeneb, A.K.; Seydim, A.C. Use of ozone in the food industry *Lebensm.-Wiss. u.-Technol.* **2004**, 37, 453–460

Halvarson, H. Quantitative gas chromatographic analysis of micro amounts of volatile carbonyl compounds via their DNPH derivatives *Journal of Chromatography A* **1971**, 57, 406–409

Hamdaoui, O. Dynamic sorption of Methylene Blue by cedar sawdust and crushed brick in fixed bed columns *Journal of Hazardous Materials B* **2006**, 138, 293–303

Hsing, H.J.; Chiang, P.C.; Chang, E.E.; Chen, M.Y. The decolorization and mineralization of Acid Orange 6 azo dye in aqueous solution by advanced oxidation processes: A comparative study *Journal of Hazardous Materials* **2007**, 141, 8–16

Huang, Y.H.; Huang, Y.F.; Huang, C.; Chen, C.Y. Efficient decolorization of azo dye Reactive Black B involving aromatic fragment degradation in buffered Co^{2+}/PMS oxidative processes with a ppb level dosage of Co^{2+}-catalyst *Journal of Hazardous Materials* **2009**, 170, 1110–1118

Iglesias, J.; Gallardo, J.M. and Medina, I. Determination of carbonyl compounds in fish species samples with solid-phase microextraction with on-fibre derivatization *Food Chemistry* **2010**, 123, 771–778

Karaca, S.; Gurses, A.; Acıkyıldız, M.; Ejder, M. Adsorption of cationic dye from aqueous solutions by activated carbon Microporous and Mesoporous Materials **2008**, 115, 376–382

Kluwe, W.M.; Montgomery, C.A.; Giles, H.D. and Prejean, J.D. Encephalopathy in rats and nephropathy in rats and mice after subchronic oral exposure to benzaldehyde *Food and Chemical Toxicology* **1983**, 21, 245–250

Koyuncu, K.; Afsar, H. Decomposition of dyes in the textile wastewater with ozone *Journal of Environmental Science and Health* **1996**, A31, 1035–1041

Koziel, J.A.; Noah, J.and Pawliszyn, J. Field sampling and determination of formaldehyde in indoor air with solid-phase microextraction and on-fiber derivatization *Environ. Sci. Technol.* **2001**, 35, 1481–1486.

Le Lacheur, R.M.; Sonneneberg, L.B.; Singer, P.C.; Christman, R.F.; Charles, M.J. Identification of carbonyl compounds in environmental samples *Environ. Sci. Technol.* **1993**, 27, 2745–2753

Lin, H.; Ye, Q.; Deng, C.; Zhang, X. Field analysis of acetaldehyde in mainstream tobacco smoke using solid-phase microextraction and a portable gas chromatograph *Journal of Chromatography A* **2008**, 1198–1199, 34–37

Maljaei, A.; Arami, M.; Mahnoodi, N.M. Decolorization and aromatic ring degradation of colored textile wastewater using indirect electrochemical oxidation method *Desalination* **2009**, 249, 1074–1078

Ma, T.H. and Harris, M.M. Review of the Genotoxicity of formaldehyde *Mutation res.* **1988**, 196, 37–59

Martos, P.A. and Pawliszyn, J. Sampling and determination of formaldehyde using solid-phase microextraction with on-fiber derivatization *Anal. Chem.* **1998**, 70, 2311–2320

Ortiz, R.; Hagino, H.; Sekiguchi, K.; Wang, Q.; Sakamoto, K. Ambient air measurements of six bifunctional carbonyls in suburban area *Atmospheric Research* **2006**, 82, 709–718.

Ozsoy, H.D.; Kumbur, H.; Saha, B.; van Leeuwen, J. (Hans) Use of *Rhizopus* oligosporus produced from food processing wastewater as a biosorbent for Cu(II) ions removal from the aqueous solutions *Bioresource Tech.* **2008a**, 99, 4943–4948

Ozsoy, H.D.; van Leeuwen, J. (Hans); Koziel, J.A.; Esplugas, M.; Onuki, S.; Mumm, L. Investigating alternative adsorbents and other techniques for color removal Iowa State U. Report to Gen Mills, Sep, **2008b**

Ozsoy, H.D.; van Leeuwen, J. (Hans) Pb (II) Ions Removal by Dried *Rhizopus* oligosporus Biomass Produced from Food Processing Wastewater, Chapter 18 In: Fluid Waste Disposal, Environmental Science, Engineering and Technology Series, Nova Publishers ISBN: 978-1-60741-915-, **2010a**

Ozsoy, H.D.; van Leeuwen, J. (Hans) Removal of color from fruit candy waste by activated carbon adsorption *J. Food Eng.* **2010b**, 101, 106–112

Pang, X.; Mu, Y.; Yuan J. and He, H. Carbonyls emission from ethanol-blended gasoline and biodiesel-ethanol-diesel used in engines *Atmospheric Environment* **2008**, 42, 1349–1358

Pawliszyn, J. Solid Phase Microextraction: Theory and Practice, Wiley-VCH, ISBN: 0471190349, **1997**

Parshetti, G.K.; Telke, A.A.; Kalyani, D.C.; Govindwar, S.P. Decolorization and detoxification of sulfonated azo dye methyl orange by Kocuria rosea MTCC 1532 *Journal of Hazardous Materials*, **2010**, 176, 503–509

Possanzini, M.; Di Palo, V; Cecinato, A. Evaluation of lower carbonyls andphotochemical oxidants by HPLC-UV and HRGC-MS *Atmospheric Environment* **2003**, 37, 1309–1316

Possanzini, M.; Di Palo, V.; Brancaleoni, E.; Frattoni, M.; Ciccioli, P. A train of carbon and DNPH-coated cartridges for the determination of carbonyls from C1 to C12 in air and emission samples *Atmospheric Environment* **2000**, 34, 5311–5318

Richardson, M.L. Dyes - The Aquatic Environment and the Mess made by Metabolites *Journal of the Society of Dyers and Colourists* **2008**, 99, 198–200

Saison, D.; De Schutter, D.P.; Delvaux, F.; Delvaux, F.R. Determination of carbonyl compounds in beer by derivatisation and headspace solid-phase microextraction in combination with gas chromatography and mass spectrometry *Journal of Chromatography A* **2009**, 1216, 5061–5068

Satsumabayashi, H.; Kurita, H.; Chang, Y.; Carmichael, G.R. Photochemical formations of lower aldehydes and lower fatty acids under long-range transport in central Japan *Atmospheric Environment* **1995**, 29, 255–266

Schmarr, H.; Potouridis, T.; Ganß, S.; Sang, W.; Kopp, B.; Bokuz, U.; Fischer, U. Analysis of carbonyl compounds via headspace solid-phase microextraction with on-fiber derivatization and gas chromatographic–ion trap tandem mass spectrometric determination of their O-(2,3,4,5,6-pentafluorobenzyl)oxime derivatives *Analytica Chimica Acta.* **2008**, 617, 119–131

Schmarr, H.; Sang, W.; Ganß, S.; Fischer, U.; Köpp, B.; Schulz, C.; Potouridis, T. Analysis of aldehydes via headspace SPME with on-fiber derivatization to their O-(2,3,4,5,6-pentafluorobenzyl)oxime derivatives and comprehensive 2D-GC-MS *J. Sep. Sci.* **2008**, 31, 3458 – 3465

Sladek, N.E.; Manthey, C.L.; Maki, P.A.; Zang Z. and Landkamer, G.J. Xenobiotic oxidation catalyzed by aldehyde dehydrogenases Drug, *Metab. Rev.* **1989**, 20, 697–720

Sowinski, P.; Wardencki, W.; Partyka, M. Development and evaluation of headspace gas chromatography method for the analysis of carbonyl compounds in spirits and vodkas *Analytica Chimica Acta.* **2005**, 539, 17–22

Stashenko, E.E.; Mora, A.L.; Cervantes, M. and Martínez, J.R. HS–SPME Determination of Volatile Carbonyl and Carboxylic Compounds in Different Matrices *Journal of Chromatographic Science* **2006**, 44, 347–353

Tang, W.Z. and An, H. UV/TiO_2 Photocatalytic Oxidation of Commercial Dyes in Aqueous Solutions *Chemosphere* **1995a**, 31, 4157–4170

Tang, W.Z. and An, H. Photocatalytic Degradation Kinetics and Mechanism of Acid Blue 40 by TiO_2/UV in Aqueous Solution *Chemosphere* **1995b**, 31, 4171–4183

Til, H.P.; Woutersen, R.A.; Feron, V.J. and Clary, J.J. Evaluation of the oral toxicity of acetaldehyde and formaldehyde in a 4-week drinking-water study in rats *Food Chem., Toxicol.* **1988**, 26, 447–452

Trenholm, R.A.; Rosario-Ortiz F.L. and Snyder, S.A. Analysis of formaldehyde formation in wastewater using on-fiber derivatization–solid-phase microextraction–gas chromatography–mass spectrometry *Journal of Chromatography A* **2008**, 1210, 25–29

Tsai, S.W. and Chang, C.M. Analysis of aldehydes in water by solid-phase microextraction with on-fiber derivatization *Journal of Chromatography A* **2003**, 1015, 143–150

Tsai, S.W.; Kao, K.Y. Diffusive sampling of airborne furfural by solid-phase microextraction device with on-fiber derivatization *Journal of Chromatography A* **2006**, 1129, 29–33

US Environmental Protection Agency, Determination of carbonyl compounds in drinking water by pentafluorobenzylhydroxylamine derivatization and capillary gas chromatography with electron capture detection, Office of Research and Development, US EPA, Method 556, **1998**

Van Leeuwen, J.; Sridhar, A.; Esplugas, M.; Onuki, S.; Cai, L.; Harrata, A.K. and Koziel, J.A. Improving biodegradation of organic pollutants with ozonation during biological wastewater treatment *Ozone Sci. & Eng.* **2009a**, 31, 63–70

Van Leeuwen, J.; Sridhar, A.; Esplugas, M.; Onuki, S.; Cai, L. and Koziel, J.A. Ozonation within an activated sludge system for azo dye removal by partial oxidation and biodegradation *Ozone Sci. & Eng.* **2009b**, 31, 279–286

Van Leeuwen, J.; Badriyha, B. and Vaczi, S. Investigation into ozonation of coal coking processing wastewater for cyanide, thiocyanate and organic removal *Ozone Sci. & Eng.* **2003a**, 25, 273-83

Van Leeuwen, J.; Pipe-Martin, C. and Lehmann, R. The South Caboolture Water Reclamation Process *Ozone Sci. & Eng.* **2003b**, 25, 107-120

Villanueva-Rodríguez, M.; Hernández-Ramírez, A.; Peralta-Hernández, J.M.; Bandala, E.R.; Quiroz-Alfaro, M.A. Enhancing the electrochemical oxidation of acid-yellow 36 azo dye using boron-doped diamond electrodes by addition of ferrous ion *Journal of Hazardous Materials* **2009**, 167, 1226–1230

Vimonses, V.; Lei, S.; Jin, B.; Chow, C.W.K.; Saint, C. Kinetic study and equilibrium isotherm analysis of Congo Red adsorption by clay materials *Chemical Engineering Journal* **2009**, 148, 354–364

Wu, J. and Wang, T. Effects of some water-quality and operating parameters on the decolorization of reactive dye solutions by ozone *Journal of Environmental Science and Health* **2001**, A36, 1335–1347

Wu, J.; Eiteman, M.A.; Law, S.E. Evaluation of membrane filtration and ozonation processes for treatment of reactive dye wastewater *Journal of environmental engineering* **1998**, 124, 272–277

Wu, J.; Doan, H.; Upreti, S. Decolorization of aqueous textile reactive dye by ozone *Chemical Engineering Journal* **2008**, 142, 156–160

Yu, J.; Jeffries, H.E.; Sexton, K.G. Atmospheric photooxidation of alkylbenzenes – I. carbonyl product analysis *Atmospheric Environment* **1997**, 31, 2261–2280

Zhang, H.; Duan, L.; Zhang, D. Decolorization of methyl orange by ozonation in combination with ultrasonic irradiation *Journal of Hazardous Materials* **2006**, B138, 53–59